University of Zagreb
Faculty of Sciences

Saša Ilijić

Spectral Disentangling of Close Binary Stars

Submitted to the Department of Physics
for the degree of Master of Science (Physics)

Zagreb, 2003

Contents

Chapter 1

Introduction

1.1 The role of close binary stars

The physics of close binary stars is much more complicated than that of single stars. Due to gravitational interaction the component stars are tidally distorted. The mutual irradiation of the atmospheres heats the portions facing one another to higher temperatures. On a long time scale the evolution of a component of a binary system differs from that of a single star of similar mass. Tidal distortions induce faster mixing of the material in the stellar interior which affects the chemical evolution of the star. The volume of space that a star can occupy is limited by the geometry of the system. When a component of a binary star expands due to stellar evolution matter may be transferred to the other component resulting in a contact or a semidetached configuration.

Despite of their complexity, the binary stars are sometimes said to be 'the royal road to the stars'. The components serve one to another as probes. The double-lined spectroscopic binaries, and in particular the eclipsing ones, play an especially important role. Through combined modeling of the light curves and measurements of the radial velocities during the orbital cycle accurate masses and radii can be determined. The possibilities extend even to studying the distribution of mass within the components stars through the analysis of the apsidal motion in binary stars with eccentric orbits.

Over the past two decades several new methods for analysis of close binaries were developed. In some of them the concepts from other fields of application, such as tomography or maximum entropy image reconstruction, were utilized to extract as much information as possible from a single time dependent point source on the sky. On the other hand, methods initially developed through the work on binary stars played crucial roles in recent

detections of planets orbiting stars.

1.2 Separation and disentangling of the composite spectra, description of the problem

The term *close binary star* is most frequently used to designate a system consisting of two stars that are close enough to affect each others evolution. Such systems are not visible binaries, i.e. the two light sources cannot be directly resolved even with the most powerful telescopes, nor can the spectra of component stars be recorded separately. This is as well true for many well-detached systems that might not fall into the category of close binary stars defined as above. Even some visual binaries, which can be separated photometrically, may not allow the spectra of components to be recorded separately. In all such systems, unless the luminosities of the components of the binary star differ greatly, the spectrum that can be recorded consists of the spectral features of both components and is called the *composite spectrum*. A time series of such spectra well distributed over the orbital cycle contains information on:

- the dependence of the radial velocities of the component stars on the orbital phase, and
- spectral features of component stars.

In almost all cases, this information is 'entangled', and is difficult to extract. The spectral lines blend to form shapes that can not be analyzed as such.

Measurements of radial velocities in the composite spectra are required for the determination of the masses of the component stars. Simple methods such as fitting Gaussians into well resolved lines, and not so simple methods such as cross-correlation techniques are considered to be standard RV-measurement tools. But such measurements are in general hampered by a number of difficulties, e.g. line blending, large rotation, component confusion, signal-to-noise ratio, etc. Big advance has been achieved through the application of the cross-correlation technique, but even this method suffers from drawbacks, the need for template spectra being the most serious one.

The spectra of component stars are needed if the surface temperatures are to be determined or if the abundances of chemical elements in the stellar atmospheres are to be studied. The techniques based on 'spectral subtraction', i.e. on subtracting the spectral features of an assumed spectral type

can be applied, but at the risk of biasing the results if inadequate templates are used. These difficulties motivated the development of more objective techniques.

Spectral separation: Given a time series of composite spectra, and corresponding radial velocities and light contributions of the component stars, this technique reconstructs the spectra of component stars. This technique does not make use of any a-priori information on the spectral features in the component spectra.

Spectral disentangling: This is an extension to the spectral separation technique where in addition to component spectra we determine a reasonably selected subset of the parameters of the binary system, usually the parameters of orbit.

The fundamental difference when compared to predecessors is that these techniques do not require the use of spectral templates. They are, however, computationally intensive, and their performance improves with the size and the quality of the data set.

1.3 The most important solutions

The first successful reconstruction of component spectra that did not rely on spectral templates was the tomographic separation of AO Cas by Bagnuolo & Gies (1991). In this work the radial velocities of component stars were measured by the cross-correlation technique. The reconstruction was carried out through an iterative least-squares technique and was named 'the tomographic separation of composite spectra'. The technique was successfully applied in a series of works by the same group, see Gies et al. (2002) and references therein.

Simon & Sturm (1994a) implemented the separation technique using the singular value decomposition technique to handle the large scale linear least squares problem. More importantly they introduced the disentangling technique by optimizing the radial-velocity semi-amplitudes of the component stars. The earliest applications of the technique are by Simon & Sturm (1994b) and by Simon et al. (1994).

Hadrava (1995) proposed to use discrete Fourier transforms of the spectra in order to uncouple the large system of linear equations. This resulted in a computationally very simple and robust separation and disentangling technique, albeit with some limitations compared to the predecessors. This technique has seen many successful applications, e.g. by Hensberge et al. (2000) or

by Griffin (2002). Hadrava (1995) proposed to use the separation technique to treat higher multiplicity systems, as well as to optimize the light-variability related parameters through disentangling procedures (Hadrava 1997).

1.4 Aim of this work

The motivation to undertake the revision of the concepts behind the spectral separation and disentangling techniques came from the work of Hensberge, Pavlovski and Verschueren (2000) on the binary star V578 Mon. They applied the disentangling technique to determine the radial velocity semi-amplitudes and to reconstruct the spectra of the component stars. Echelle spectra with merged orders obtained with the CASPEC spectrograph on the 3.6 m telescope at ESO were used. Despite of the successful application of the fore-mentioned technique it was realized that deeper understanding of some of its aspects is required for the planned future work in this field. In particular, this applies to:

- propagation of errors into the component spectra and parameters of orbit, and
- normalization of the component spectra obtained through separation.

Furthermore, the code used during the work on V578 Mon could handle only very short stretches of spectra compared to the spectral region covered by the echelle spectrograms. It was therefore decided to build the disentangling code from scratch and to start error analysis work.

I start by reviewing the concepts behind the spectral separation techniques in the Chapter 2 of this work. The 'wavelength-domain' approach by Simon & Sturm (1994a) and the 'Fourier-domain' approach by Hadrava (1995) are discussed in detail. I also present the matters of normalization of the component spectra obtained through spectral separation that are currently understood. The error analysis work is still under way and some of the results are published elsewhere (Ilijić, Hensberge & Pavlovski 2001a,b). In the Chapter 3 of this work the disentangling method is applied to the spectra of the hot binary star V453 Cyg. The Fourier-based disentangling code that I wrote has already been used by Griffin (2002) and is described in the Chapter 4. The Appendix A deals with the equations of the orbital motion that are of importance in the context of disentangling of the composite spectra. A procedure for physically correct normalization of the component spectra obtained through the separation technique is proposed in Appendix B.

Chapter 2

Formulation of the methods

In the first Section of this Chapter I introduce the mathematical model of the spectra of the binary star in terms of functions of a continuous variable. This model is the basis of the spectral separation and disentangling techniques. In the following three Sections I deal with the mathematical properties of the problem of separation of composite spectra. A very general formulation is given in Section 2.2 in order to prepare the grounds for the approximations that are introduced later. Section 2.3 deals with the 'wavelength domain' separation that was historically first introduced and has proven itself useful in practice. Section 2.4 covers the 'Fourier domain' separation that speeds up the computation. Section 2.5 addresses currently well understood sources of apparent misbehaviour of the component spectra obtained through separation and gives procedures for bringing them into the 'expected' form. The disentangling method is introduced in Section 2.6 as an application of the separation technique. Propagation of random error in the input quantities to the results of separation and disentangling is briefly covered in Section 2.7.

2.1 The model of the composite spectrum

A composite spectrum of a binary star is the spectrum of the summed lights of component stars. The concept straightforwardly generalizes to composite spectra of stellar systems with higher order of multiplicity. Whenever the component stars of a multiple stellar system are not be resolved individually, only the composite spectra can be recorded. A simple mathematical model of the composite spectra can be formulated using the following assumptions:

1. The component stars of a multiple stellar system perform orbital motion around the center of mass of the system. Observed radiation of

each component is therefore Doppler-shifted according to the time dependent radial velocity of the component.

2. The spectra of the component stars are time independent apart from the above mentioned Doppler-shift and an overall intensity factor introduced to account for possible distortions of the star and/or eclipses.

3. The time series of composite spectra of the stellar system is recorded by a spectrograph with linear response in intensity and at resolution sufficient to resolve the spectral features of interest as well as the Doppler shifts due to orbital motion. Exposure time is negligible compared to the timescale on which the change in the orbital radial velocities could be detected. The recorded spectrum is free of the effects of absorption in the interstellar medium or the atmosphere of the Earth, or any other systematic effects. Random photon-shot noise is present in the spectra.

The first assumption is valid in all cases of interest and should not be viewed as an approximation. For the functional dependence of the radial velocities on time in case of a binary system see Appendix A. The assumption 2 is the key assumption for application of the method. It is, however, an approximation and only as long as it is acceptable it makes sense to apply the method. The assumption 3 is an idealization needed not to over-complicate the formulation that follows.

The stellar spectrum is, for practical reasons, usually understood as the product of two functions. One is the smooth function with the dimension of the flux known as the 'continuum' and the other is the dimensionless function that describes all short-scale structure in the spectra (spectral lines), known as the 'normalized spectrum'. Where there are no spectral lines the normalized spectrum is unity. In accord with this I use the notation $F(\lambda) = \bar{F}(\lambda)f(\lambda)$ where $F(\lambda)$ is the stellar flux and $\bar{F}(\lambda)$ and $f(\lambda)$ are the continuum and the normalized spectrum respectively.

I begin by expressing the composite spectra in terms of the spectra of component stars as continuous functions, not including the random noise. I use the symbol Y for the composite spectra and X for the component spectra throughout this text. Index k loops over the component stars. Index j loops over the times t_j when the composite spectra were observed. Therefore:

$$Y_j(\lambda) = \sum_k \epsilon_{kj} X((1 - \beta_{kj})\lambda) \ , \tag{2.1}$$

where ϵ_{kj} is the *eclipse factor* to star k at time t_j. The eclipse factor for a spherically symmetric star out of eclipse is unity. During ingress, egress, or

partial eclipse $0 < \epsilon < 1$, and in total eclipse $\epsilon = 0$. Eclipse factors may be used to introduce brightness changes due to tidal distortions of the stars. β_{kj} is the radial velocity of the star k at time t_j here in units of the speed of light. Making use of our notation (2.1) expands to:

$$\bar{Y}_j(\lambda) y_j(\lambda) = \sum_k \epsilon_{kj} \bar{X}_k((1-\beta_{kj})\lambda) x_k((1-\beta_{kj})\lambda) \ . \tag{2.2}$$

As this holds for any component spectra it also holds for $x_k(\lambda) = 1$ (no lines) in particular. In this case I expect $y_j(\lambda) = 1$. It follows:

$$\bar{Y}_j(\lambda) = \sum_k \epsilon_{kj} \bar{X}_k((1-\beta_{kj})\lambda) \ . \tag{2.3}$$

Substituting (2.3) into (2.2):

$$y_j(\lambda) = \sum_k \ell_{kj}(\lambda) x_k((1-\beta_{kj})\lambda) \ , \tag{2.4}$$

where:

$$\ell_{kj}(\lambda) = \frac{\epsilon_{kj} \bar{X}_k((1-\beta_{kj})\lambda)}{\sum_l \epsilon_{lj} \bar{X}_l((1-\beta_{lj})\lambda)} \ . \tag{2.5}$$

The function $\ell_{kj}(\lambda)$ specifies the fractional contribution of the continuum of the component k at t_j to the continuum of the composite spectrum at wavelength λ. The equation (2.4) relates the normalized composite spectra to the normalized spectra of component stars.

2.2 The general formulation

The next step is to replace the continuous representation of the spectra by the discrete representation, and to include the random noise. If the composite spectrum $y_j(\lambda)$ observed at t_j is sampled at the grid of N_j wavelength points λ_{ji}, $i = 1, \ldots, N_j$, I can write:

$$y_{ji} = \rho \sigma_{ji} + y_j(\lambda_{ji}) \tag{2.6}$$

where ρ is a random number drawn from a unit variance normal distribution and σ_{ji} is the uncertainty of a particular measurement. The second term on the right hand side must as well be written in the discrete form:

$$y_{ji} = \rho \sigma_{ji} + \sum_k \ell_{kji} \hat{x}_k((1-\beta_{kj})\lambda_{ji}, \{x_{k\alpha}\}) \tag{2.7}$$

where $\ell_{kji} = \ell_{kj}(\lambda_{ji})$ and the function $\hat{x}_k(\lambda_{ji}, \{x_{k\alpha}\})$ estimates the amplitude of the component spectrum k from a set of M_k parameters $x_{k\alpha}$, $\alpha = 1, \ldots, M_k$, at wavelength λ. The equation (2.7) can be viewed as having the observed data on its left hand side and the mathematical model on the right hand side.

The function $\hat{x}_k(\lambda_{ji}, \{x_{k\alpha}\})$ deserves several comments. The extent to which it will be able to reproduce the continuous function $x_k(\lambda)$ at each wavelength depends on the way it is defined and on the number of parameters it is uses. The errors originating from the inability of $\hat{x}_k(\lambda_{ji}, \{x_{k\alpha}\})$ to reproduce $x_k(\lambda)$ are considered to be negligible compared to uncertainties in the data. Choosing the parameters $x_{k\alpha}$ to represent the amplitudes at a grid of wavelength points $\lambda_{k\alpha}$, $\alpha = 1, \ldots, M_k$, is certainly the simplest way of defining the function $\hat{x}$. More importantly, this choice makes $\hat{x}$ linear in $x_{k\alpha}$.

Let me now, in addition to assumptions 1–3, introduce the following assumptions:

- The observed composite spectra of a stellar system show blends of spectral features of $N_\star \geq 2$ stars orbiting around their center-of-mass.
- A time series consisting of $N_{\rm obs}$ composite spectra is observed. The exposure times t_j, $j = 1, \ldots, N_{\rm obs}$, are well distributed over the orbital cycle(s).
- The radial velocity of the star k, $k = 1, \ldots, N_\star \geq 2$, at the time t_j, $j = 1, \ldots, N_{\rm obs}$, is known for each k and j and is labeled β_{kj}
- The fractional contribution of the continuum of the star k to the continuum of the composite spectrum observed at t_j at wavelength λ_{ji} is known and is labeled $\ell_{kji} = \ell_{kj}(\lambda_{ji})$.
- The function $\hat{x}_k(\lambda_{ji}, \{x_{k\alpha}\})$ that represents the spectrum of the component of the stellar system is linear in the parameters $x_{k\alpha}$.

It follows that (2.7) represents a set of $\sum_{j=1}^{N_{\rm obs}} N_j$ equations linear in $\sum_{k=1}^{N_\star} M_k$ parameters $x_{k\alpha}$. This system of equations can be solved for $x_{k\alpha}$ which means that *the normalized spectra of component stars are reconstructed.* However, the system of equations must be well posed. There should be more equations than unknowns which is fulfilled if $N_{\rm obs} > N_\star$ and $M_k \simeq N_j$, although this alone is not a sufficient condition for well-posedness.

An over-determined system of linear equations, especially when modeling real data is not expected to have an exact solution. Rather, for the system $\mathbf{A} \cdot \mathbf{x} = \mathbf{y}$, where $\mathbf{A}$ has more rows than columns (i.e.. more equations

than unknowns), the so called 'least squares solution' is required such that it minimizes the quantity $r = |\mathbf{A} \cdot \mathbf{x} - \mathbf{y}|$. In our case the set of equations that is being solved is:

$$\frac{y_{ji}}{\sigma_{ji}} = \frac{1}{\sigma_{ji}} \sum_k \ell_{kji} \hat{x}_k((1-\beta_{kj})\lambda_{ji}, \{x_{k\alpha}\}) \; , \tag{2.8}$$

so that the minimized quantity is:

$$r^2 = \sum_{j=1}^{N_{\rm obs}} \sum_{i=1}^{N_j} \frac{1}{\sigma_{ji}^2} \left(y_{ji} - \sum_{k=1}^{N_\star} \ell_{kji} \hat{x}_k((1-\beta_{kj})\lambda_{ji}, \{x_{k\alpha}\}) \right)^2 \; , \tag{2.9}$$

The parameters $x_{k\alpha}$ can, therefore, be considered as free parameters in a large scale least-squares fit of a mathematical model to observed data. However, for practical reasons it is essential that the model remains linear in the parameters.

2.3 Separation in the wavelength domain

The general formulation of the separation technique of the preceding Section has not yet proven itself useful in practical applications. Rather than that, a much simpler and therefore more limited formulation is used. The most important simplifications are the following:

- While the general formulation allows each composite spectrum to be sampled on its own grids of wavelength points and does not require any regularity in sampling, the simple formulation requires all composite spectra to be sampled on the same grid of wavelength points equidistant in the logarithm of the wavelength. This choice allows the Doppler shifts to be expressed in number of data-bins independently of the position in the spectrum. The same grid is also used for the resulting component (model) spectra.

- The coefficients ℓ_{kji} (fractional contribution of the continuum of component k to the continuum at time t_j at wavelength λ_{ji}) are assumed to be independent of wavelength so that the third index can be omitted. Furthermore, the time dependence is frequently neglected so that only first index remains. They are simply called *light-factors*.

- The measurement uncertainties are considered equal for all amplitude points of a composite spectrum. This is equivalent to assigning fitting weights to the full wavelength region of the composite spectra, and not to individual amplitudes.

With minor differences these apply to the 'tomographic separation' of Bagnuolo & Gies (1991), to the 'wavelength domain separation' of Simon & Sturm (1994a) as well as to the 'Fourier domain separation' of Hadrava (1995).

Let us consider the 'wavelength domain separation' in some detail. The problem is formulated as an over-determined system of linear equations. The N composite (observed) spectra contain the same number of data points and are thought of as vectors $\mathbf{y}_j$, $j = 1, \ldots, N$. They are concatenated into one long vector $\mathbf{y}$ that will be on the r.h.s. of (2.10). The l.h.s. consists of a matrix, $\mathbf{A}$, multiplying a vector, $\mathbf{x}$, that is defined as concatenation of the two (or more) spectra of component stars, $\mathbf{x}_k$, $k = 1, 2$. The matrix $\mathbf{A}$ consists of blocks, $\mathbf{A}_{jk}$, each responsible of transferring the amplitudes of one component spectrum into one of the composite spectra. The block $\mathbf{A}_{jk}$ transfers $\mathbf{x}_k$ into $\mathbf{y}_j$ taking into account both β_{kj} and ℓ_{kj}. The system of equations (2.8) can be written as:

$$\begin{pmatrix} \mathbf{A}_{11} & \mathbf{A}_{12} \\ \vdots & \vdots \\ \mathbf{A}_{N1} & \mathbf{A}_{N2} \end{pmatrix} \cdot \begin{pmatrix} \mathbf{x}_1 \\ \mathbf{x}_2 \end{pmatrix} = \begin{pmatrix} \mathbf{y}_1 \\ \vdots \\ \mathbf{y}_N \end{pmatrix} \tag{2.10}$$

or $\mathbf{A} \cdot \mathbf{x} = \mathbf{y}$ in short. The observed data is on the r.h.s. in the vector $\mathbf{y}$ while the β_{kj} and ℓ_{kj}, that are assumed to be known, are used to construct the matrix $\mathbf{A}$. Solving (2.10) for $\mathbf{x}$ requires the inverse of $\mathbf{A}$. Since $\mathbf{A}$ is not a square matrix, and since it may be rank deficient, the recommended technique for computing the inverse makes use of the singular value decomposition (Simon & Sturm 1994a). Note that this formulation straightforwardly extends to include more than two component spectra.

Thanks to logarithmic binning in wavelength, equal spectral resolutions in data and the model and uniform weighting of data points in the fit the structure of blocks $\mathbf{A}_{jk}$ is particularly simple. Basically these are diagonal matrices with the diagonal shifted according to β_{kj} and multiplied by ℓ_{kj}. An example setup of (2.10) is shown in Figure 2.1. Four composite spectra, each 11 data bins long, are modeled by two model spectra. Note that the vectors $\mathbf{x}_k$ must be somewhat longer than the vectors $\mathbf{y}_j$ in order to provide the amplitudes to the r.h.s. under different Doppler shifts (the β_{kj}). Consequently the blocks $\mathbf{A}_{jk}$ must have more columns than rows (for the shifting 'diagonal' not to fall off the edge of the block). The values of β_{kj} and ℓ_{kj} used in Figure 2.1 are:

$$(\beta_{kj}) = \begin{pmatrix} 1 & 0 & -2 & -1 \\ -2 & 0 & 4 & 2 \end{pmatrix} \quad \text{and} \quad (\ell_{kj}) = \begin{pmatrix} \frac{2}{3} & \frac{1}{2} & \frac{2}{3} & \frac{2}{3} \\ \frac{1}{3} & \frac{1}{2} & \frac{1}{3} & \frac{1}{3} \end{pmatrix} \tag{2.11}$$

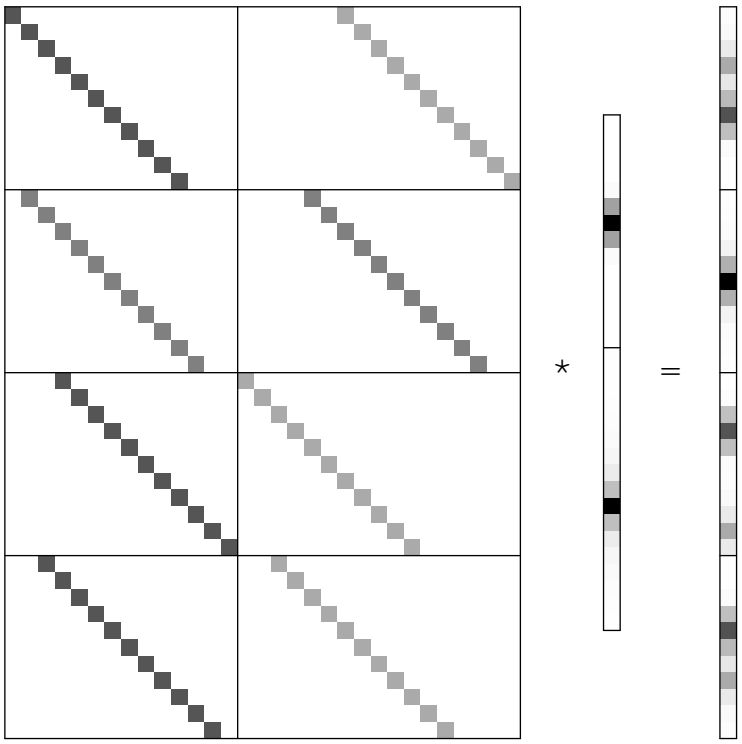

Figure 2.1: Density plot of the matrix equation (2.10). The blocks $\mathbf{A}_{jk}$ and the sub-vectors $\mathbf{x}_k$ and $\mathbf{y}_j$ are separated by lines. Gray-scale spans from zero (*white*) to unity (*black*) within the matrix, and reverse within the vectors. See also (2.11).

where β_{kj} are given in the number of data bins. For simplicity the β_{kj} were kept at integral values. At non-integral shifts the 'diagonal' is diluted to perform linear or higher order interpolation of the component spectra. Note that at $j = 2$ the radial velocities of both stars are zero, and that the star 1 contributes less light relatively to the other star due to eclipse.

In practice, due to the large size of the matrix $\mathbf{A}$, computing its inverse is a problem worth of considering. The time required by the computations sets the limit to the size of the data set that can be used in one run. The system of equations similar to the one described above has been solved in Bagnuolo & Gies (1991) by means of an iterative least squares technique. The computational time seems not to have been a concern, but a remark on problems with the numerical stability of their approach can be found in Hynes (1996). Simon & Sturm (1994a) advocate inverting the matrix by means of the singular value decomposition (Press et al. 1992; Wolfram 1991). If applied straightforwardly this requires a lot of time. Simon (2001) has succeeded to take advantage of the sparsity of $\mathbf{A}$ in order to compute the singular value decomposition in a reasonable time (apparently at the price of not being able to use the time dependent ℓ_{kj} or deferentially weighted data points). Unfortunately, his algorithm has not been published.

2.4 Separation in the Fourier domain

If there are $N_{\rm bin}$ data bins per each of the $N_{\rm obs}$ observed spectra the system of equations (2.10) consists of $N_{\rm obs} \times N_{\rm bin}$ coupled equations linear in a little more than $2N_{\rm bin}$ unknowns for a binary system (or $N_\star \times N_{\rm bin}$ in general). Using the discrete Fourier transforms (DFTs) of the data the system of equations can be uncoupled into $\frac{1}{2}N_{\rm bin} + 1$ systems of $N_{\rm obs}$ complex equations involving only two unknowns for a binary (or $N_\star$ in general). The use of DFT in the context of the separation of the composite spectra was first proposed by Hadrava (1995).

The discrete Fourier transform (DFT) of a string of amplitudes a_i, $i = 0, \ldots, N-1$, where N is even, is defined as:

$$\tilde{a}_n = \frac{1}{N} \sum_{i=0}^{N-1} \mathrm{e}^{-\frac{2\pi \mathrm{i}}{N} n i} a_i \ , \quad n = -\frac{N}{2} + 1, \ldots, \frac{N}{2} \ . \tag{2.12}$$

Choosing n to range from $-N/2 + 1$ to $N/2$ is a matter of a convention ($\tilde{a}_n$ are periodic with period N) as is the choice of the normalization constant and of the sign of the argument of the exponential function. The DFT amplitude $\tilde{a}_n$ is said to correspond to frequency $\omega_n = 2\pi n/N$. The DFT

amplitude $\tilde{a}_0$ corresponding to 'zero frequency' is recognized as the average of the amplitudes a_i. The $\tilde{a}_{N/2}$ corresponds to the highest frequency not equivalent to some lower frequency that is known as the critical or Nyquist frequency. Note that for real amplitudes a_i it holds $\tilde{a}_{-n} = \tilde{a}_n^*$. The inverse transform of (2.12) is:

$$a_i = \sum_{n=-N/2+1}^{N/2} \mathrm{e}^{\frac{2\pi\mathrm{i}}{N} in} \tilde{a}_n \ , \quad i = 0, \ldots, N-1 \tag{2.13}$$

The normalization and the sign of the argument of the exponential function are in accord with the choice taken in (2.12).

A simple 'theorem' reads that multiplying $\tilde{a}_n$ by $\mathrm{e}^{\frac{-2\pi\mathrm{i}}{N}\beta n}$ is equivalent to shifting the a_i by β places toward right:

$$\begin{aligned} a'_i &= \sum_{n=-N/2+1}^{N/2} \mathrm{e}^{\frac{2\pi\mathrm{i}}{N} in} \left(\mathrm{e}^{\frac{-2\pi\mathrm{i}}{N}\beta n} \tilde{a}_n \right) \\ &= \sum_{n=-N/2+1}^{N/2} \mathrm{e}^{\frac{2\pi\mathrm{i}}{N}(i-\beta) n} \tilde{a}_n \\ &= a_{i-\beta} \ . \end{aligned} \tag{2.14}$$

As all amplitudes shift by the same number of bins I can use this expression to write the Doppler shifts of spectra sampled equidistantly in the logarithm of the wavelength. It is therefore possible to write the equation analogous to (2.10) in terms of DFTs of the observed composite spectra $\tilde{y}_{jn}$, $j = 1, \ldots, N_{\mathrm{obs}}$, and the component spectra $\tilde{x}_{kn}$, $k = 1, \ldots, N_\star$, $n = -N_{\mathrm{bin}}/2 + 1, \ldots, N_{\mathrm{bin}}/2$:

$$\sum_{k=1}^{N_\star} \ell_{kj} \mathrm{e}^{-\frac{2\pi\mathrm{i}}{N_{\mathrm{bin}}}\beta_{kj} n} \tilde{x}_{kj} = \tilde{y}_{jn} \ , \quad j = 1, \ldots, N_{\mathrm{obs}} \ , \tag{2.15}$$

where β_{kj} are the shifts expressed in the number of data bins and ℓ_{kj} are light factors. The system (2.15) consists of N_{obs} equations linear in $N_\star$ unknowns. For each $n = 0, \ldots, N_{\mathrm{bin}}/2$ the system (2.15) can be solved independently, i.e. the system (2.10) is now uncoupled. Note that for $n < 0$ the system (2.15) is the complex conjugate of the corresponding system with $n > 0$, so only one has to be solved. (Also note that for $n = 0$ and for $n = N_{\mathrm{bin}}/2$ the system (2.15) is purely real.) Each of the systems is over-determined if $N_{\mathrm{obs}} > N_\star$, but may still not have a unique solution, see Section 2.5. The use of singular value decomposition for calculating the inverse of the matrix is recommended by Ilijić et al. (2001b).

The eq. (2.15) is easily modified to include measurement uncertainties assigned to composite spectra as whole. It suffices to divide its both sides with σ_j, the 'average' measurement uncertainty assigned to the amplitudes y_{ji}. Solving the system is then equivalent to minimizing:

$$r_n^2 = \sum_{j=1}^{N_{\rm obs}} \frac{1}{\sigma_j^2} \left(\tilde{y}_{jn} - \sum_{k=1}^{N_\star} \ell_{kj} \mathrm{e}^{-\frac{2\pi \mathrm{i}}{N_{\rm bin}} \beta_{kj} n} \tilde{x}_{kn} \right)^2 \tag{2.16}$$

for each n independently. However, uncertainties cannot be assigned to individual amplitudes of y_{ji} any more since they were already taken with equal weights when $\tilde{y}_{jn}$ was computed.

The most important advantage of the 'Fourier domain' approach over the 'wavelength domain' approach considered in Section 2.3 is the significantly smaller CPU time requirement. Instead of solving one large system of $N_{\rm obs} \times N_{\rm bin}$ equations in (approximately) $N_\star \times N_{\rm bin}$ unknowns as in (2.10), using (2.15) I am solving $N_{\rm bin}/2+1$ small complex (all but two) systems consisting of $N_{\rm obs}$ equations in $N_\star$ unknowns. Assuming that time required to compute the inverse of an $M \times N$ matrix goes as $(MN)^{\gamma/2}$ the advantage of the DFT approach goes as $N_{\rm bin}^{\gamma-1}$. Adopting $\gamma = 3$ for a square matrix (Press et al. 1992), this is $N_{\rm bin}^2$, so it is not surprising that the 'Fourier domain' separation was chosen for treating data sets with $N_{\rm bin} \approx 16000$ as in Griffin (2002).

The discrete Fourier transforms of the composite spectra must be calculated before (2.15) can be used, and the inverse transform must be applied to the results after-wards. The price of calculating the transforms varies strongly in $N_{\rm obs}$. It is high for prime numbers and cheap for powers of 2 (Johnson & Frigo 1999), but is usually not a concern. Particularly in disentangling procedures (see Section 2.6) where many separations must be calculated during the optimization process, and the result does not have to be brought to wavelength domain after each separation, calculating the DFTs pays off.

The serious drawback unavoidably introduced by the DFT is that it understands the model spectra of the component stars as periodic functions (Ilijić et al. 2001a,b). If a string of amplitudes is shifted by multiplying its DFT by the exponential factor as in (2.14) the amplitudes that are pushed out through one end re-enter through the other. This nonphysical feature of the model may lead to the inability of the model to reproduce the data even when the latter is completely in accord with the assumptions 1–3 of Section 2.2. The effect is most pronounced at the ends of the spectral range and is therefore called 'end of range effect' (ERE), but it propagates all over the spectral region that is processed. Particular care must be taken when choosing the spectral range that is to be processed in order to make ERE

negligible. A rule of thumb is to cut the composite spectra in the middle of regions of continuum that are at least twice as wide as the radial velocity semi-amplitude of the least massive star. Furthermore, the continuum should be at the same level at both ends.

2.5 The degrees of freedom

Remarks on the mathematical indeterminacies in the component spectra reconstructed through separation techniques appear since Bagnuolo et al. (1992). There are setups of β_{kj} and ℓ_{kj} such that the mathematical solutions to (2.10) or (2.15) nonetheless exist, but do not resemble the spectra of the stars. Partial ill posedness of the system of equations may lead to non-physical degrees of freedom in the component spectra that are either

- used to obtain a better fit to the data,
- or, if they are not capable of improving the fit, they are just initialized to non-physical values (according to some mathematical convention).

If component spectra are subject to such degrees of freedom this *must be taken into account* if attempting physical interpretation. Most applications of spectral separation were carried out assuming equal light contributions of both component stars in all composite spectra that were used. Such a setup, known as the 'no light variability' case, is more than any other prone to problems. Although at present only incomplete understanding of the indeterminacies in the systems of equations and the resulting degrees of freedom in the spectra can be offered, I continue the discussion because of its practical importance. The discussion will be limited to the 'no light variability' case.

Assuming equal light contribution of the two component stars to all the composite spectra the light factors ℓ_{kj} reduce to ℓ_k. The basic indeterminacy introduced by this assumption is most evident in the 'Fourier domain' formulation. Let us consider the system of equations (2.15) for $n = 0$ (frequency zero). This system is purely real and it deals with the averages of the amplitudes in the spectra. It can be written in matrix form as:

$$\begin{pmatrix} \ell_1 & \ell_2 \\ \vdots & \vdots \\ \ell_1 & \ell_2 \end{pmatrix} \cdot \begin{pmatrix} \tilde{x}_{10} \\ \tilde{x}_{20} \end{pmatrix} = \begin{pmatrix} \tilde{y}_{10} \\ \vdots \\ \tilde{y}_{N0} \end{pmatrix} \tag{2.17}$$

There are more equations than unknowns so I am requiring the least squares solution. But it is evident that if $(\tilde{x}_{10}, \tilde{x}_{20})$ is the least squares solution, than

so is also any solution of the form $(\tilde{x}_{10}+\ell_2 c, \tilde{x}_{20}-\ell_1 c)$, where c is an arbitrary real constant. In such situations, according to a mathematical convention, one chooses the shortest length solution defined as the one that minimizes $\tilde{x}_{10}^2+\tilde{x}_{20}^2$. Let us carry this out with uncertainties included as in (2.16). The least squares requirement leads to:

$$\ell_1\tilde{x}_{10}+\ell_2\tilde{x}_{20}=\frac{\sum_j \sigma_j^{-2}\tilde{y}_{j0}}{\sum_j \sigma_j^{-2}}\ , \tag{2.18}$$

which is undetermined. The shortest length requirement picks one solution out of infinity of least squares solutions:

$$\begin{pmatrix} \tilde{x}_{10} \\ \tilde{x}_{20} \end{pmatrix} = \frac{\sum_j \sigma_j^{-2}\tilde{y}_{j0}}{(\ell_1^2+\ell_2^2)\sum_j \sigma_j^{-2}} \begin{pmatrix} \ell_1 \\ \ell_2 \end{pmatrix}\ . \tag{2.19}$$

This is obviously not a physical result, since the averages in the normalized component spectra are by no means proportional to the assumed light ratio. I must not consider the shortest length result as unique. It is only a mathematically correctly initialized solution. The solution including the degree of freedom is:

$$\begin{pmatrix} \tilde{x}_{10} \\ \tilde{x}_{20} \end{pmatrix} = \frac{\sum_j \sigma_j^{-2}\tilde{y}_{j0}}{(\ell_1^2+\ell_2^2)\sum_j \sigma_j^{-2}} \begin{pmatrix} \ell_1 \\ \ell_2 \end{pmatrix} + \text{const.} \begin{pmatrix} \ell_2 \\ -\ell_1 \end{pmatrix} \tag{2.20}$$

Technically, if solving a system like (2.17) using singular value decomposition one automatically obtains the least squares shortest length solution, while the more traditional techniques, such as normal equations, might simply break down complaining on a singular matrix. Note that (2.15) being singular for $n=0$ does not imply that (2.15) is singular for $n>0$. In Appendix B a simple procedure is formulated that proposes running separation with the so called 'generic' light factors and adjusting the solution to the assumed (trial) light ratio after-wards. The procedure takes into account the 'additive constant' degree of freedom.

In practical work, especially if using long stretches of spectra, the 'additive constant' is not the only way the component spectra misbehave. The spectra 'bend' on a scale much longer than the radial velocity semi-amplitudes of the component stars. Bending is not without regularity, where one component goes up the other goes down, which suggests that I should look more carefully for additional indeterminacies in the sets of equations. An attempt went as follows:

The component spectra $x_k(u)$, where $u = \ln\lambda$ and $k = 1, 2$, can be written using the Taylor expansion in the neighbourhood of the point u_0:

$$x_k(u) = \sum_{n=0}^{\infty} \frac{x_k^{(n)}(u_0)}{n!}(u - u_0)^n \ . \tag{2.21}$$

In a binary system with the mass ratio $q = m_1/m_2$ the time dependent Doppler shifts can be written as:

$$\beta_{1,2}(t) = a_{1,2}\beta(t) \qquad \text{where} \qquad \frac{a_2}{a_1} = -q \tag{2.22}$$

where $a_{1,2}$ are the radial velocity semi-amplitudes (in $\ln\lambda$ units) and $\beta(t)$ is a single time dependent function. The composite spectrum at u_0 follows as:

$$\begin{aligned} y(u_0) &= \sum_{k=1,2} \ell_k x_k(u_0 + a_k\beta) \\ &= \sum_{k=1,2} \ell_k \sum_{n=0}^{\infty} \frac{x_k^{(n)}(u_0)}{n!}(a_k\beta)^n \ . \end{aligned} \tag{2.23}$$

I now look for two spectra $\xi_{1,2}(u)$ such that if added to $x_{1,2}$ they do not affect the l.h.s. of the above equation. If these exist then they represent the true degrees of freedom in $x_{1,2}$. They should obey:

$$0 = \sum_{n=0}^{\infty} \left(\sum_{k=1,2} \ell_k \frac{\xi_k^{(n)}(u_0)}{n!} a_k^n \right) \beta^n \tag{2.24}$$

for any β. If this expansion is cut off at some n I end up with a polynomial in β, and if the latter is to vanish at any β its coefficients must all be equal to zero. It follows:

$$\frac{\xi_1^{(n)}(u_0)}{\xi_2^{(n)}(u_0)} = -\frac{\ell_2}{\ell_1}\left(\frac{a_2}{a_1}\right)^n = (-1)^{n+1}\frac{\ell_2}{\ell_1}q^n \tag{2.25}$$

For $n = 0$ and $n = 1$ this is:

$$\frac{\xi_1(u_0)}{\xi_2(u_0)} = -\frac{\ell_2}{\ell_1} \qquad \text{and} \qquad \frac{\xi_1'(u_0)}{\xi_2'(u_0)} = \frac{\ell_2}{\ell_1}q \tag{2.26}$$

The first condition is equivalent to (2.20). The second condition tells that if there are slopes in ξ_1 and ξ_2 they are of the same sign. But if these two conditions are fulfilled at some u_0, they cannot be fulfilled at any other. Therefore we must conclude that slopes in the component spectra are not

part of the true degrees of freedom in the 'no light variability' solution. And as the slopes are not allowed, I need not look at higher derivatives.

The most I can do at present to remove the 'bends' from the component spectra is to extend the relation (2.20) by replacing the constant by a smooth 'slowly' variable function of u.

$$\begin{pmatrix} x_1(u) \\ x_2(u) \end{pmatrix}_{\text{adjusted}} = \begin{pmatrix} x_1(u) \\ x_2(u) \end{pmatrix}_{\text{best fit}} + f(u) \begin{pmatrix} \ell_2 \\ -\ell_1 \end{pmatrix} \tag{2.27}$$

Unfortunately, it still remains unclear how slowly $f(u)$ must vary in u before it starts spoiling the fit significantly, or what is most appropriate mathematical form of $f(u)$.

2.6 Disentangling of the composite spectra

Disentangling of composite spectra is an application of the spectral separation technique that is not directed only toward reconstructing of the spectra of component stars, but also toward determining the parameters of orbit of the stellar system. The technique was introduced by Simon & Sturm (1994a), see also Sturm (1994) for details.

In Sections 2.3 and 2.4 I was assuming that the correct light factors ℓ_{kj} and the radial velocities β_{kj} are known for each component spectrum (k) in each composite spectrum that is being used (j). I could say that the coefficients β_{kj} and ℓ_{kj} determine the entangling of the component spectra in the composite spectra, and that faithful reconstruction of the component spectra from the composite spectra is possible only if these coefficients are known. Light-factors can be determined through the analysis of the light curves and the radial velocities can be directly measured in the composite spectra by means of the traditional techniques such as fitting of Gaussians into the well-resolved lines or by two-dimensional cross-correlation with the template spectra. While the separation of composite spectra can be carried out within the 'no-light-variability' assumption even without a-priori knowledge on the light-ratio (see Appendix B), inaccurately determined radial velocities seriously affect the reconstruction of the component spectra. Accurate radial velocities can therefore be considered the second most critical part of the data, first being the composite spectra, needed to reconstruct the spectra of the individual components of the stellar system.

Disentangling is a procedure that applies spectral separation to the composite spectra of a binary without a-priori requiring complete knowledge of the 'entangling' coefficients, but rather considering them the free parameters of the fit. It is based on a reasonable assumption that the fit of the model to

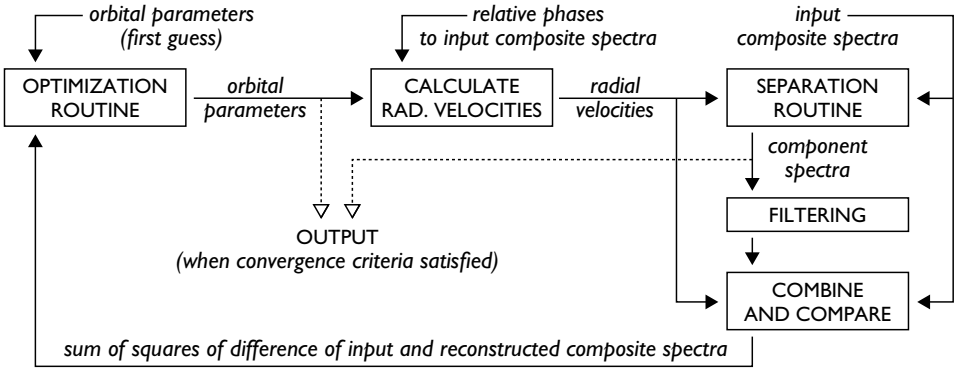

Figure 2.2: The flowchart of the disentangling procedure.

the data obtained through spectral separation is better if the radial velocities are accurate. The measure of the 'goodness of fit' is the usual weighted sum of the squares of the residuals of model and the data. In the wavelength domain formulation (2.10) this is simply $||\mathbf{A}\cdot\mathbf{x}-\mathbf{y}||$, while in case of the Fourier formulation this is according to (2.16):

$$r^2 = \sum_{n=1}^{N_{\rm bin}/2}\sum_{j=1}^{N_{\rm obs}}\frac{1}{\sigma_j^2}\left(\tilde{y}_{jn}-\sum_{k=1}^{N_\star}\ell_{kj}\mathrm{e}^{-\frac{2\pi\mathrm{i}}{N_{\rm bin}}\beta_{kj}n}\tilde{x}_{kn}\right)^2 \qquad (2.28)$$

(the $n=0$ term was omitted because it is independent of β_{kj}). The principal difference is that now the 'entangling coefficients' ℓ_{kj} and possibly β_{kj} as well, are free parameters of the fit. The model is still linear in $\tilde{x}_{kn}$, but it is non-linear in ℓ_{kj} and possibly β_{kj}. To preserve the computational efficiency the strategy for minimizing r^2 is therefore divided into two levels, non-linear and linear. A general purpose multidimensional optimization routine is applied on the small number of non-linear parameters and separation is calculated for each setup of these parameters as described in Sections 2.3 and 2.4. The flowchart of the procedure is depicted in Fig. 2.2.

An attempt to optimize the radial velocities β_{kj} directly adds $N_{\rm obs}\times N_\star$ free parameters to the model. Although this number is not large compared to the number of free parameters in the linear part, the free β_{kj} contribute tremendously to the flexibility of the model. As a result the disentangling procedure is likely to be unstable. A reasonable way out of this pitfall is to constrain the β_{kj} by the applicable physical laws. For a well-detached binary system, where proximity and vicinity effects can be neglected, the solution to the Kepler problem provides the functional dependence of the radial velocities on time. For an overview of the equations of the orbital motion in

a binary system see Appendix A. Therefore, instead of optimizing $2N_{\rm obs}$ radial velocities in a binary system, one chooses to optimize a suitably chosen combination of the parameters of orbit. In most applications to eclipsing binaries the ephemeris is known to high accuracy and epochs are assigned to the spectrograms. In circular orbit the radial velocity semi-amplitudes $K_{1,2}$ might be the only free parameters in the fit, while for an eccentric orbit the eccentricity, the longitude of periastron, and an overall phase shift might be the additional free parameters.

2.7 Progression of random noise

Several works agree that, at least in principle, random error in the input quantities does not influence the results of separation and disentangling in a systematic way (Simon & Sturm 1992; Sturm 1994; Hynes 1996; Hynes & Maxted 1998; Ilijić et al. 2001a,b). But there are also several warnings that the separation and disentangling techniques might introduce systematic effects if not used carefully. The matter is quite difficult to trace analytically and the analyzes are based on processing of the simulated data.

The most convincing demonstration of the spectral separation technique at its time was the application to the double lined eclipsing binary V453 Cyg (Simon & Sturm 1994a). The spectrum of the fainter component obtained through separation of eight out-of-eclipse composite spectra was shown to match the spectrum recorded during the totality of the secondary eclipse. This result is partly reproduced in Chapter 3.

A useful empirical formula relating the rms scatter of the amplitudes of the reconstructed component spectra to the rms of the amplitudes in the composite spectra is proposed in Ilijić et al. (2001a):

$$\sigma_{1,2} \approx \frac{\sigma_{\rm input}}{\ell_{1,2}\sqrt{N_{\rm obs}-2}} \ . \tag{2.29}$$

This result has shown to be valid for different values of $N_{\rm obs}$, $\sigma_{\rm input}$ and $\ell_{1,2}$ through Monte Carlo simulations where disentangling was applied to 200 equivalent realizations of a particular synthetic data set. The mean reconstructed spectra showed no systematic effects apart of end-of-range effects introduced by the Fourier-based separation routine.

In Ilijić et al. (2001b) sets of 400 equivalent realizations of (only) four composite spectra were subjected to separation using known 'entangling parameters'. Fig. 2.3 shows that the Fourier based separation introduced no systematic effects in the reconstructed spectra. Care was taken to place the ends of the spectral regions into continuum regions as wide as I could find

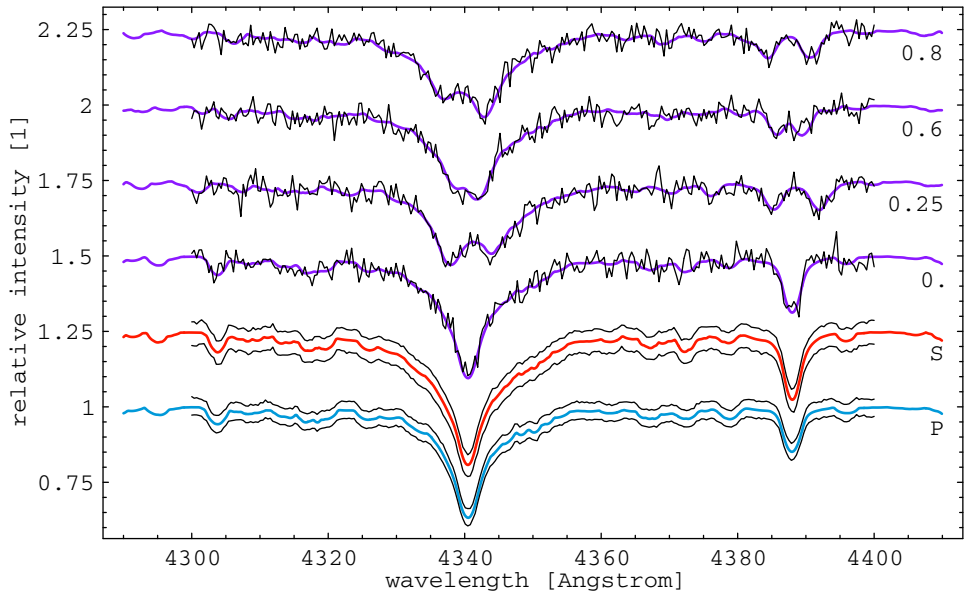

Figure 2.3: Fourier domain separation: spectral region around Hγ and He I lines, $\beta_{\rm grid} = 25$ km s^{-1}, $S/N = 40$. Two synthetic component spectra (*blue and red lines labeled P and S*) are combined into composite spectra (*violet lines labeled with orbital phase*). 400 artificial data sets are created (*one shown in black*) and subjected to separation. The resulting $\pm 1\sigma$ region is shown (*black lines*). All spectra are plotted on the same scale; shift $\frac{1}{4}$ is applied among spectra for clarity.

them. On the other hand in the setup of Fig. 2.4 one of the ends was intentionally not placed in a continuum region. This is one of the causes of the systematic effects in the spectra obtained through Fourier domain separation, the other being the 'blemish' in the composite spectra artificially introduced as an static absorption feature at 4096 Å. The spectra obtained through wavelength domain separation are free of bias. The wavelength domain separation is as such not susceptible to end-of-range effects, and the possibility of assigning measurement uncertainty to each data point independently was used to 'mask off' the narrow spectral region affected by the static absorption feature.

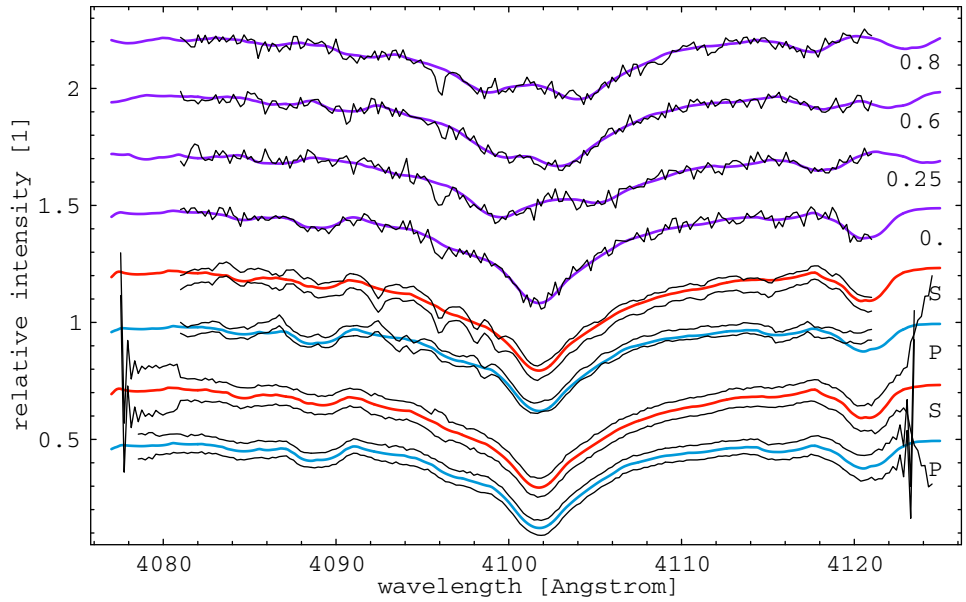

Figure 2.4: Wavelength domain vs. Fourier domain separation: spectral region around Hδ line, $\beta_{\rm grid} = 15$ km s^{-1}, $S/N = 50$. Note the 'blemish at 4096 Å. The $\pm 1\sigma$ regions obtained with wavelength domain separation (*the bottom two spectra*) and with Fourier domain separation (*the next two spectra*) are shown (see also caption to Figure 2.3).

Chapter 3

Application to V453 Cyg

Simon & Sturm (1994a) chose the double lined eclipsing binary star V453 Cyg as the test system when they were introducing the spectral disentangling technique. The spectrum that they obtain for the brighter component matches the spectrum observed during the totality of the secondary eclipse. In this Chapter the Fourier-based separation routine is shown to pass the same test on the same data. The observed spectra used in Simon & Sturm (1994a) were kindly provided to me by Dr. Klaus Simon. In the first Section I summarize the basic facts about V453 Cyg. In Sections 3.2 and 3.3 I present the observed spectra of V453 Cyg and show how they were prepared for Fourier-based separation. In Section 3.4 I discuss the application of the disentangling technique and compare the radial velocity semiamplitudes that I obtain to the results published in the literature. In Section 3.5 I carry out the separation in two different ways. The renormalization procedure of Appendix B, based on the results of Section 2.5, is applied step-by-step to show that it leads to correctly normalized spectra of component stars.

3.1 The massive binary system V453 Cyg

V453 Cygni or HD227696, $\alpha = 301\overset{\circ}{.}645698$, $\delta = 35\overset{\circ}{.}740632$ (J2000) is a massive, detached, eclipsing, double-lined binary star, a member of the open cluster NGC 6871. The variability of V453 Cyg was discovered by Wachmann (1939). The light curve shows an annular and a total eclipse, and was observed and analyzed by Cohen (1971, 1974) and by Wachmann (1973, 1974). The annular eclipse is deeper (primary) than the total eclipse (secondary) from which it follows that the larger star is the hotter star. To avoid any confusion throughout this text I will be referring to the stars as the brighter (B) and the fainter (F), keeping in mind that during the total eclipse F is

eclipsed by B.

The system was found to exhibit apsidal motion with the period of $P_{\rm aps} =$ 71 years at an orbital eccentricity of about $e \simeq 0.02$ by (Wachmann 1974). Unfortunately, the only recently observed and published time of minimum that I could find (Bíró 1998) is not in line with this orbital solution. Radial velocities of components of V453 Cyg were measured by Popper & Hill (1991). As already mentioned, the spectra were disentangled by Simon & Sturm (1994a).

In a disentangling procedure one tries to fix as many parameters of orbit as possible so that as few as possible remain to be optimized. For V453 Cyg the only parameter of orbit that is well determined is the orbital (sidereal) period. According to Cohen (1974):

$$T_{\rm Min.I} = {\rm HJD}\, 2439340.0988 + 3\overset{\rm d}{.}8898128E\ . \tag{3.1}$$

However, because of the apsidal motion and of the uncertainties I must not rely on the above ephemeris for prediction of the times of the minima at epochs much different from the epochs of the observations that were used to establish this result. Another input that is required for the separation technique to produce the correct results is the phase and wavelength dependence of the light-ratio of the system. For all spectra of V453 Cyg taken out of eclipse I adopt the result of Wachmann (1974):

$$L = \frac{\ell_{\rm B}}{\ell_{\rm F}} = 2.66667\ . \tag{3.2}$$

The wavelength dependence of the light ratio will not be considered because the spectral types are not very different and a fairly short spectral range will be treated.

3.2 Spectra of V453 Cyg

Eight spectra of V453 Cyg were obtained by Fiedler and Sturm with a coude-spectrograph and a 2.2 m telescope at the Calar Alto Observatory in July 1992. Seven of these were taken out of eclipse and one was taken during the totality of the secondary eclipse (see Table 3.1). The spectra cover the range of 4290–4510 Å at the resolution of $\simeq 0.2$ Å/px (1024 pixels in total). The data reduction was completed by the observers and I received the wavelength calibrated and continuum normalized spectra. The only operation on the data that I applied was the correction to the radial velocities and the dates of the mid-exposures to account for motion of the Earth around the Sun. I calculated parameters for these corrections using SkyCalc (Thorstensen 2000).

Table 3.1: The observed spectra of V453 Cyg. The epoch is calculated according to (3.1).

Label	HJD 2448810+	$T_{\mathrm{exp.}}$ [s]	Epoch 2430+	Note
a	1.489869	1200	4.922	
b	2.480025	1200	5.177	
c	3.424391	1200	5.419	
d	4.472093	900	5.689	
e	6.531810	1200	6.218	
f	7.651999	1500	6.506	tot. ecl.
g	8.474703	900	6.718	
h	8.615600	900	6.754	

3.3 Preparation of the spectra for disentangling

The epochs in Table 3.1 are calculated using the ephemeris (3.1). As all eight spectra were recorded within less than two successive orbital cycles of the binary system any inaccuracy in the determination of the period will not significantly affect the relative consistency in the assignment of the orbital phases. The error in the period may, however, accumulate over time and lead to erroneous prediction of the times of minima. In our case this results in a phase shift which is of no concern in the disentangling procedure because the phase shift can be used as a free parameter. The distribution of the spectra over the orbital cycle is shown in Figure 3.1.

In order to apply the Fourier domain separation to a time series of composite spectra they must be sampled on identical grids of wavelength points equidistantly distributed in the logarithm of the wavelength. I decided to use a grid with the radial-velocity resolution of $\beta_{\mathrm{grid}} = 10\ \mathrm{km\,s^{-1}/bin}$ which is somewhat higher than the resolution of the detector. Linear interpolation of the data was used during re-sampling. The ends of the spectral range must be placed so that the end-of-range effects are reduced as much possible (see Sect. 2.4) The vertical lines on the Fig. 3.1 show my choice. The resulting number of data points per spectrum is $N_{\mathrm{bin}} = 1344$.

I assigned the light factors to the seven out-of-eclipse spectra according to (3.2):

$$\ell_{\mathrm{B}} = \frac{L}{L+1} = 0.7273 \quad \text{and} \quad \ell_{\mathrm{F}} = \frac{1}{L+1} = 0.2727 \tag{3.3}$$

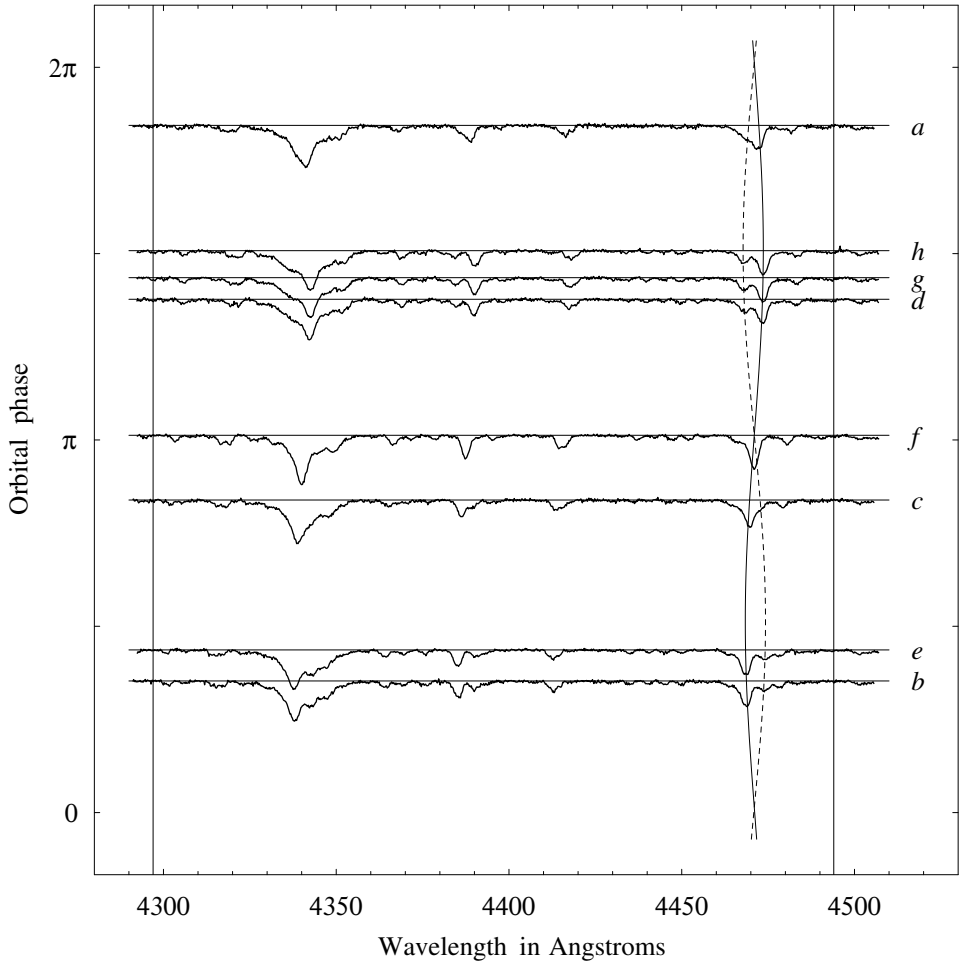

Figure 3.1: The distribution of the observed spectra of V453 Cyg over the orbital cycle (see Table 3.1). The RV curves obtained through disentangling are shown for the He I 4471 Å line core of the brighter component (*solid*) and of the fainter component (*dashed*). The vertical lines in the background show the wavelength-cuts that are used for the Fourier-domain separation (4297 Å–4494 Å).

Table 3.2: The jackknife procedure of estimating the bias in the parameters of orbit determined through disentangling. The longitude of periastron ω applies to the brighter star (B).

Run label	$K_{\rm B}$ [km s^{-1}]	$K_{\rm F}$ [km s^{-1}]	μ_0 [deg]	e	ω [deg]	$\mu_0+\omega$ [deg]
skip a	174.16	214.64	71.903	0.0303	16.878	
b	173.09	217.54	89.434	0.0139	−1.886	
c	173.35	214.49	38.669	0.0475	50.334	
d	174.80	218.14	75.676	0.0169	12.465	
e	176.05	215.80	65.520	0.0127	22.634	
f	174.38	215.64	55.204	0.0505	32.269	
g	174.49	216.33	53.317	0.0260	34.799	
h	173.91	214.12	59.513	0.0185	28.520	
use all	174.48	216.27	59.442	0.0225	28.674	88.116
$\sigma_{\rm JACK}$	2.33	3.77	40.150	0.0385	40.687	1.314

and for the in-eclipse spectrum (f) where the fainter component is totally eclipsed I put $\ell_{\rm B}=1$ and $\ell_{\rm F}=0$. Light factors assigned like this are used when all eight composite spectra are used for separation. If the in-eclipse spectrum (f) is omitted the no-light-variability assumption applies (see Sect. 2.5) and all light-factors are reset to the generic value of $\ell_{\rm gen}=1/2$ (see Appendix B).

3.4 The parameters of orbit

The expected radial velocity amplitudes (see Table 3.3) are $K_{\rm B,F}\sim 200$ km s^{-1} and according to Wachmann (1974) the eccentricity of orbit is $e\simeq 0.02$. The departure of the radial velocities in a low eccentricity orbit from the nearest circular approximation is approximately given by (A.19) which evaluates to ~ 4 km s^{-1}. The accuracy of the RV measurements is hopefully below this value so I consider the circular approximation potentially harmful. Unfortunately, due to its uncertainty, I may not safely extrapolate the orbital solution of Wachmann (1974) until the time of the spectrograms, and I am forced to leave five parameters of an eccentric orbit as free parameters (see Sect. A).

With eight observed spectra the radial-velocity curve is constrained at eight points. Taking into account that it is has five degrees of freedom there

Table 3.3: The radial velocity semi-amplitudes of the brighter ($K_{\rm B}$) and of the fainter ($K_{\rm F}$) component of V453 Cyg.

Source	$K_{\rm B}$ $[{\rm km\,s^{-1}}]$	$K_{\rm F}$ $[{\rm km\,s^{-1}}]$	Method
Popper & Hill 1991	171.0 ± 1.5	222.0 ± 2.5	cross-correlation
Simon & Sturm 1994a	171.7 ± 2.9	223.1 ± 2.9	disentangling
Burkholder et al. 1997	173.2 ± 1.3	213.6 ± 3.0	fitting Gausians
This work	174.5 ± 2.3	216.3 ± 3.8	disentangling

is basis for expecting unstable orbital solutions. To test the stability of the orbital solution I applied the procedure known as the jackknife estimate of bias (Efron 1982). Having eight spectra in total there are eight different ways of disentangling of only seven spectra at a time. The results of such runs are shown in the upper part of the Table 3.2. The scatter of these results around the result that is obtained using all eight spectra determines the jackknife estimate of bias. My results are shown in the lower part of the Table 3.2. It is clear that the eccentricity e, mean anomaly at zero epoch μ_0 and the longitude of periastron ω are weakly determined. The radial velocity semi-amplitudes are well determined. Table 3.3 compares the results of this work to the published results. Note that the quantity $\mu_0 + \omega$, that plays the role of an overall phase shift, is well determined. Application of the jackknife procedure to $\mu_0 + \omega$ gives the value of $88\overset{\circ}{.}1 \pm 1\overset{\circ}{.}3$.

3.5 The spectra of component stars

Once the parameters of orbit are optimized I can look at the spectra of the component stars. If the eight composite spectra are used with light factors assigned as in (3.3) the component spectra that I obtain are correctly normalized ready for spectroscopic diagnostics. The latter are shown in Figure 3.2, upper panel. The match of the model spectrum of the brighter component (B) and the spectrum observed during the totality of the secondary eclipse *(f)* is convincing as it was in Simon & Sturm (1994a). The quality of the fit of the model to all eight composite spectra can be examined in the Figures 3.4 and 3.5.

It must be noted that this example is fairly non-typical. On one occasion, while the fainter star was totally eclipsed, the spectrum of the brighter star was directly observed. and, in principle, one does not need the separation

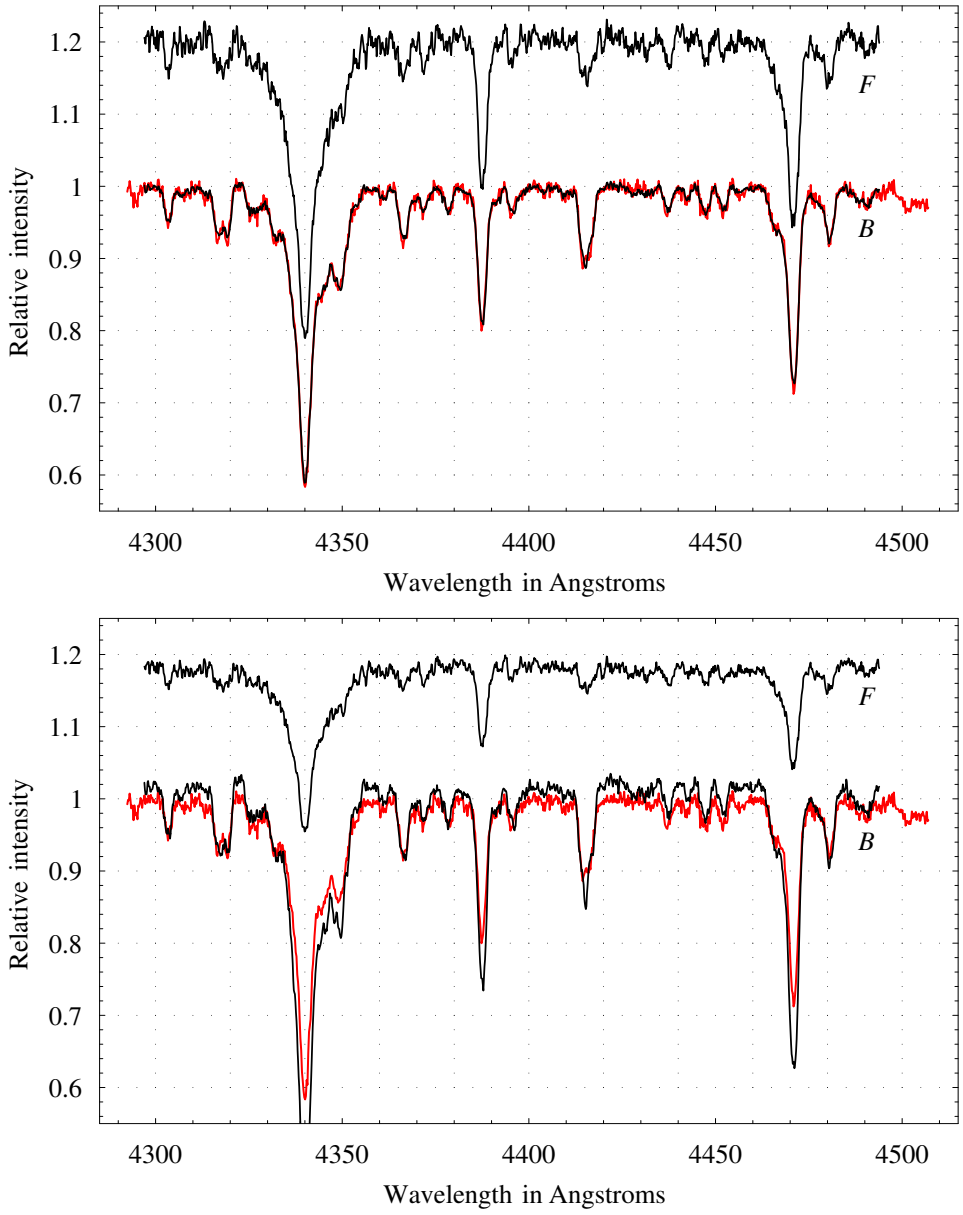

Figure 3.2: *Upper panel:* The model spectra for the brighter (B) and for the fainter (F, shifted by 0.2) component of V453 Cyg (*black*) as obtained through spectral separation using all eight observed spectra and the light-factors as in (3.3). The spectrum observed in mid-eclipse (*red*). *Lower panel:* as the upper panel, but for the separation of the seven out-of-eclipse spectra alone. Note that a renormalisation (Appendix B) is required now where the eclipse-spectrum (f, red) no longer 'fixes' the continuum.

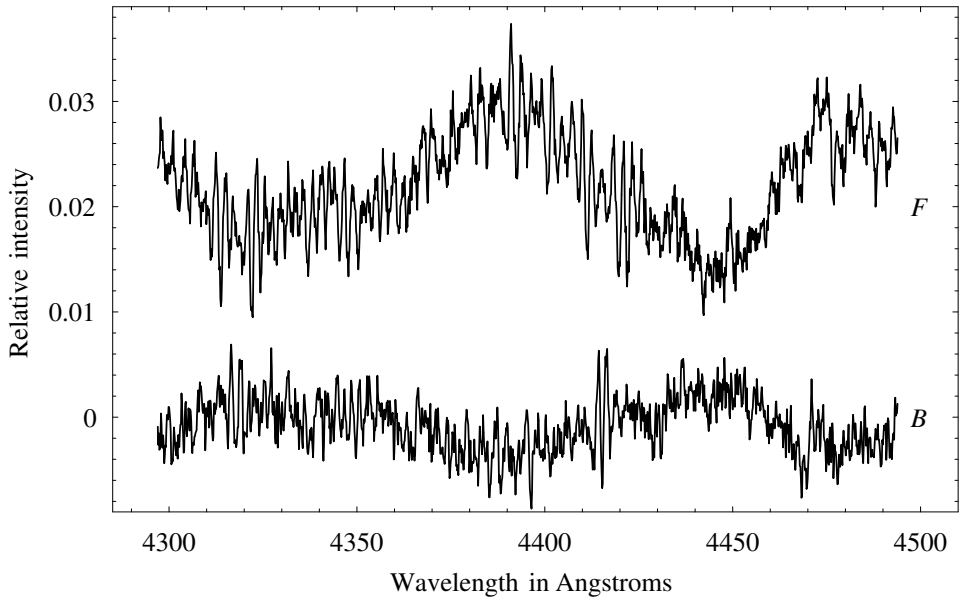

Figure 3.3: The difference of the model spectra as obtained for the brighter (B) and for the fainter (F, shifted by 0.02) component of V453 Cyg when using all eight observed spectra with light-factors and when using only the seven out-of-eclipse spectra with generic light-factors and renormalization (Appendix B).

technique to reconstruct its spectrum. But still, the separation technique uses the information available in all composite spectra and reconstructs the spectrum of the brighter component at higher signal-to-noise ratio than that of the observed spectrum.

I proceed to run the disentangling procedure using only the seven out-of-eclipse spectra. This case is, in turn, a very typical one. The no-light-variability assumption now applies and I use the generic light-factors as explained in Appendix B. The spectra z_1 and z_2 resulting from such a procedure, called quasi-spectra and shown in the Figure 3.2, lower panel, must not be interpreted as continuum normalized spectra of component stars before the renormalization procedure is carried out. I first obtain the average line blocking b from the quasi-spectra:

$$b = 1 - \frac{1}{N_{\rm bin}} \sum_{i=1}^{N_{\rm bin}} z_{1i} = 1 - \frac{1}{N_{\rm bin}} \sum_{i=1}^{N_{\rm bin}} z_{2i} = 0.041419 \qquad (3.4)$$

Next I calculate the line blocking ratio of the spectra obtained in the previous

run where all eight composite spectra were used, obtaining:

$$B = \frac{N_{\rm bin} - \sum_{i=1}^{N_{\rm bin}} x_{1i}}{N_{\rm bin} - \sum_{i=1}^{N_{\rm bin}} x_{2i}} = 1.21903 \tag{3.5}$$

In general, the value of B is obtained by trial and error, but in this case where the correct component spectra are already known, I take the opportunity to by-pass that procedure. Using the equation (B.4) I calculate the value of the free parameter c:

$$c = \frac{L-1}{L+1} - \frac{BL-1}{BL+1} b = 0.432614 \tag{3.6}$$

Finally, I use the equations (B.1) to obtain the continuum normalized component spectra.

The difference of the spectra obtained when using all eight composite spectra and light-factors and the spectra obtained from seven out-of-eclipse spectra using the renormalization procedure is shown in Figure 3.3. As can be seen, there is a correlation among the deviation of the spectra for the brighter and the fainter component. This can be corrected for through the coupled additive correction according to (2.27).

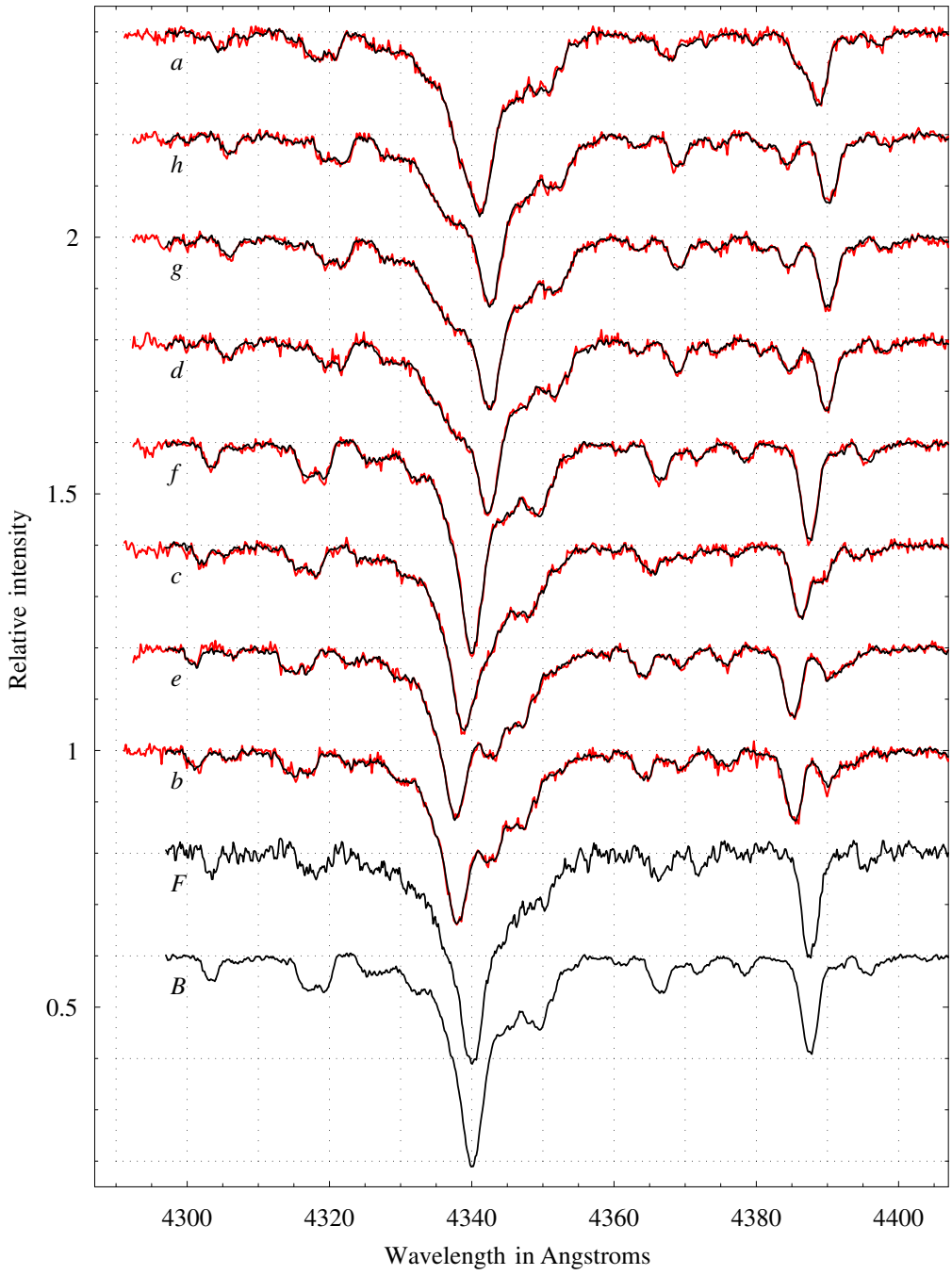

Figure 3.4: The model spectra for the brighter (B) and the fainter (F) component star and the model composite spectra (a–h) as they match the observed spectra (*red*). The observed spectra are shown in original sampling.

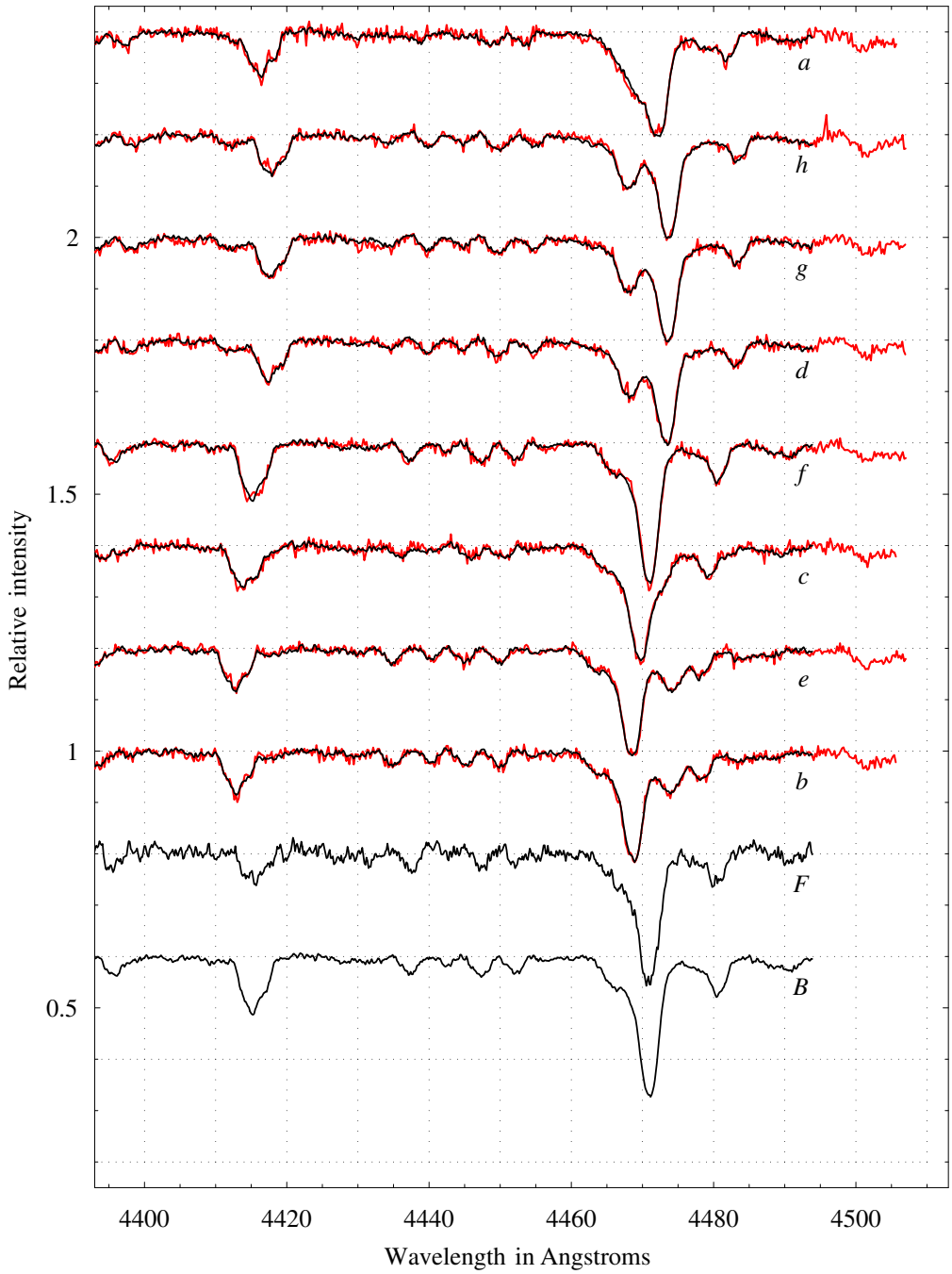

Figure 3.5: The model spectra for the brighter (B) and the fainter (F) component star and the model composite spectra (a–h) as they match the observed spectra (*red*). The observed spectra are shown in original sampling.

Chapter 4

The Code FDBinary

The code FDBINARY is a tool for separation and disentangling of composite spectra of binary stars. I wrote it with two objectives in mind. Firstly, it had to provide a flexible interface to the disentangling method in order to allow the critical error-analysis work that is still under way (Ilijić et al. 2001a,b). Secondly, in view of the real applications of the method, it had to be a stable and reliable tool. In particular it was required that the code is capable of handling large data sets such as those coming from the modern echelle spectrographs. FDBINARY operates in the Fourier domain as described in Section 2.4. The code was written in the C programming language for the UNIX operating system; it uses the routines from Johnson & Frigo (1999) and from Press et al. (1992). It has undergone only minor changes since January 2001 and has already been applied by Griffin (2002). This Chapter is an overview of the basic features of the code and can be used as a manual.[1]

4.1 Input files

All FDBINARY input files and all but one output files obey the same format. They are plain-text files containing rectangular arrays of numbers and are hereinafter referred to as *matrixfiles*. The first line has a special syntax. The first character must be a hash (`#`), then after some whitespace comes the number of data columns in the matrixfile, then after some whitespace the capital letter X, and finally, after some whitespace comes the number of data rows. The syntax of the body of the a matrixfile is very loose. Anything that follows a hash character is ignored which allows extensive commenting of the input matrixfiles. The examples in this Chapter will clarify this simple

[1]The documentation to FDBINARY was originally published on the Web:
`http://www.geof.hr/~silijic/fdbinary/refman`

concept.

The basic application of FDBINARY requires three input matrixfiles. The first matrixfile contains the continuum normalized composite spectra of the binary star. The spectra must be sampled equidistantly in the logarithm of the wavelength, all at the same resolution. The radial velocity that corresponds to one data-bin shift of a spectrum toward red is called the radial-velocity resolution of the grid and is denoted $\beta_{\rm grid}$. Preferably the spectra should be wavelength calibrated so that the radial velocity of the center of mass of the binary is the same in all spectra. The amplitudes of the spectra must be written into a matrixfile as columns, with the wavelength ascending down the file. If one uses M composite spectra sampled on the grid of N wavelength points the syntax of this matrixfile can be illustrated as follows:

$$\begin{array}{|cccc|}\hline \texttt{\#}\ M\ \texttt{X}\ N & & & \\ y_{11} & y_{21} & \cdots & y_{M1} \\ y_{12} & y_{22} & \cdots & y_{M2} \\ \vdots & \vdots & & \vdots \\ y_{1N} & y_{2N} & \cdots & y_{MN} \\ \hline \end{array} \qquad (\texttt{*.obs})$$

The tag `*.obs` indicates the required file-name suffix. where y_{ji} is the amplitude of the composite spectrum observed at epoch E_j and wavelength λ_i. Note that since the actual wavelengths are not used during the calculations they do not enter this or any other FDBINARY input matrixfile. The user has to keep record of the wavelength range independently.

The additional information on the composite spectra must be prepared in a separate matrixfile. Its syntax is:

$$\begin{array}{|ccccc|}\hline \texttt{\#\ 5\ X}\ M & & & & \\ E_1 & \gamma_1 & \ell_{11} & \ell_{21} & w_1 \\ E_2 & \gamma_2 & \ell_{12} & \ell_{22} & w_2 \\ \vdots & \vdots & \vdots & \vdots & \vdots \\ E_M & \gamma_M & \ell_{1M} & \ell_{2M} & w_M \\ \hline [P_{\rm sid}] & [\beta_{\rm grid}] & [1] & [1] & [1] \end{array} \qquad (\texttt{*.des})$$

and the required file-name suffix is `des` (for *des*criptors). The quantities in square brackets indicate the required units. The lines in this matrixfile correspond to columns in the `obs`-matrixfile. E_j is the epoch, its integral part can be left out unless apsidal motion is considered. γ_j is the center of mass radial velocity correction. A positive value should be supplied for a spectrum that is shifted toward red. Note that this does not mean that the true systemic velocity has to be known. The parameters γ_j should be used

only to remove the sub-pixel inconsistencies in radial velocity (wavelength) calibration of the spectra. The parameters ℓ_{1j} and ℓ_{2j} are the light factors, the assumed fractional contributions of the continua of the component spectra to the continuum in the composite spectrum at certain epoch. Unless they differ among the composite spectra and thus remove the first order singularity from the separation problem, it is advisable to set all light-factors to the generic value $\ell_{\rm gen} = 1/2$ and to apply the renormalization procedure (Appendix B). w_j are the fitting weights assigned to composite spectra. Typically these are set to values proportional to the square of the signal-to-noise ratio in the spectra.

The third input matrixfile specifies the initial setup of the parameters of orbit and initializes the optimization procedure. The syntax is:

`# 2 X 7`		
K_1	ΔK_1	$[\beta_{\rm grid}]$
K_2	ΔK_2	$[\beta_{\rm grid}]$
μ_0	$\Delta\mu_0$	[rad]
e	Δe	
ω_0	$\Delta\omega_0$	[rad]
ω_1	$\Delta\omega_1$	$[{\rm rad}/P_{\rm ano}]$
q	Δq	[1]

(`*.op0`)

and the required file-name suffix is `op0`. The radial-velocity semiamplitudes $K_{1,2}$ should both be supplied as positive numbers. The mean anomaly at epoch zero μ_0 and the longitude of periastron of the first star at epoch zero (or at all epochs if $\omega_1 = \Delta\omega_1 = 0$) ω_0 should be supplied in radians. Eccentricity of orbit is however $0 \leq e < 1$. The parameter ω_1 is the periastron advance in radians per anomalistic cycle in presence of apsidal motion. The parameter q is intended for the adjustment of the sidereal period relative to the value that was used to calculate the epochs. Before some experience is gathered with optimizing the period through disentangling it is strongly recommended to keep $q = \Delta q = 0$. The parameters that are to be keept fixed during disentangling should be given zero Δ-values, while the ones to optimize should be given positive Δ-values.

Input matrixfiles for FDBINARY must be given the same first part of the file-name, while the extensions must be given as as indicated above. The first part of the filename is called the *runid* and it serves as the *run-id*entifier. The FDBINARY input and output files are summarized in the table 4.1. The input and output files used for the FDBINARY runs of Chapter 3 are shown in Section 4.4

Table 4.1: The FDBINARY input and output matrixfiles. M is the number of composite spectra and N is the number of the wavelength points per spectrum. The part of the file-names indicated by * of all matrixfiles corresponding to one FDBINARY run is identical and is called the *runid*.

	file	cols	rows	contents
in:	`*.obs`	M	N	observed spectra
	`*.des`	5	M	descriptors
	`*.op0`	2	7	initial parameters of orbit
out:	`*.log`	–	–	log-file (not a matrixfile)
	`*.op1`	1	7	optimized parameters of orbit
	`*.mod`	2	N	model spectra
	`*.res`	M	N	residuals of the fit ('$o - c$')
	`*.op2`	5	M	*see text*
	`*.op3`	2	M	*see text*

4.2 Running

If the FDBINARY executable file is run without any UNIX command line arguments it will print out a short message and quit. Assuming that it can be run simply by typing its name:

```
$ fdbinary
FDBinary as of 22 Apr 2002 (eps = 2.2e-16)
FDBSEP 1C KPLREQ 07 MXFUNS 3C DHSPLX 21
```

To start a calculation the input matrixfiles must be prepared and named as explained in the preceding Section. Let me assume that the common part of the filenames, the *runid*, is simply `ecc`. The input files are:

```
$ ls
ecc.des  ecc.obs  ecc.op0
```

The command line syntax for making FDBINARY read the input files with *runid* `ecc` and perform $N_{\rm runs} = 99$ independent optimization runs is the following:

```
$ fdbinary mode=op runid=ecc nruns=99
```

There will be no output visible on the screen unless errors occur. When the calculation is done FDBINARY quits leaving behind several output files:

```
$ ls
ecc.cnd  ecc.log  ecc.obs  ecc.op1  ecc.op3
ecc.des  ecc.mod  ecc.op0  ecc.op2  ecc.res
```

As can be seen, the newly created files inherited the runid of the input files. The syntax of the output files is elaborated in the following Section.

FDBINARY calculates the least squares fit of the mathematical model discussed in detail in Section 2.4 to the data supplied through the `obs` and `des`-files. The quantity that is minimized is given by (2.28), or written out more in line with the notation of this Chapter:

$$r^2 = \sum_{n=0}^{N/2} \sum_{j=1}^{M} w_j \left(\tilde{y}_{jn} - \sum_{k=1,2} \ell_{kj} \mathrm{e}^{-\frac{2\pi \mathrm{i}}{N_{\mathrm{bin}}}(\gamma_j + \beta_{kj})n} \tilde{x}_{kn} \right)^2 \tag{4.1}$$

The $\tilde{y}_{jn}$ are the amplitudes of the discrete Fourier transform (DFT) of the observed spectra supplied in the `obs`-file, and the $\tilde{y}_{jn}$ are the DFT amplitudes of the component spectra that are being calculated. The DFTs of the observed spectra y_{jn} are, as well as the inverse-DFTs of $\tilde{x}_{kn}$, calculated internally by FDBINARY.

If one requires a separation run, i.e. if the parameters of orbit are not to be optimized, one should specify `nruns=0` on the command line, meaning 'do *no* optimization of parameters of orbit (disentangling) runs'. The radial velocities β_{kj} are computed at each epoch according to standard equations reviewed in the Appendix A, and using the parameters of orbit as supplied in the first column of the `op0`-matrixfile. (The second column of the `op0`-matrixfile is ignored if `nruns=0`.)

If any of the parameters of orbit are to be optimized one should require at least one, but preferably more than just one, optimization (disentangling) runs by specifying `nruns=`N_{runs} with $N_{\mathrm{runs}} \geq 1$. The parameters that are assigned zero Δ-values in the `op0`-file are not optimized. A positive Δ-value specifies the half-width of the range within which the initial set of 'trial points' will be distributed. For example, specifying $K_1 = 5$ and $\Delta K_1 = 1$ means that the trial points will be distributed so that $4 < K_1 < 6$. FDBINARY uses the downhill-simplex multi-dimensional non-linear optimization technique implemented as described in Press et al. (1992). As this technique is by its nature non-constrained the final solution is not necessarily located within the range that was initially assigned to the parameters. Stray orbital solutions may occur if the search wanders far away from the true solution, and there it finds a minimum of (4.1). On the other hand, the true solution may be returned even if it is not in the range that was specified to initialize the optimization. This must be kept in mind at all times because the stray solutions are likely to be found in addition to the true solution. FDBINARY uses

a random number generator to initialize each optimization run differently and independently of earlier runs. It is strongly recommended to calculate as many such independent optimization runs as is necessary to make sure that the 'best solution' is being found repeatedly. In most cases the stray solutions can be recognized as physically disallowed and disregarded. The frequency of occurrence of the stray-solutions depends on the complexity of the hyper-surface (4.1) which increases with the number of parameters that are optimized and with the sparsity of the data set.

4.3 Output files

The output file one should always inspect first is the `log`-file. It is human-readable and and mostly self-explanatory. It contains notes on most important steps of the calculation, and it reports the command line arguments that were given, and the quantities supplied in `des` and `op0` files. The contents of the `obs`-file that was used is not repeated. If $N_{\rm runs} > 0$ the parameters of orbit resulting from each optimization (disentangling) runs are reported. The tag `<<` indicates that the solution corresponded to minimum deeper than any of the minima found until then. Every time such a solution is found a set of output matrixfiles are written to disk.

The model spectra of component stars are written into a matrixfile with the extension `mod`:

2 X N
x_{11} x_{21}
x_{12} x_{22}
$\vdots$ $\vdots$
x_{1N} x_{2N}

(`*.mod`)

The residuals of the fit to the observed spectra, δ_{ji}, are written into a matrixfile with the extension `res`:

# M X N			
δ_{11}	δ_{21}	$\ldots$	δ_{M1}
δ_{12}	δ_{22}	$\ldots$	δ_{M2}
$\vdots$	$\vdots$		$\vdots$
δ_{1N}	δ_{2N}	$\ldots$	δ_{MN}

(`*.res`)

The 'observed minus calculated' convention is obeyed, so the model composite spectra can, if required, be obtained by subtracting the residuals (`res`-file) from the observed composite spectra (`obs`-file).

The optimized parameters of orbit are written into a matrixfile with the extension `op1`. The syntax of this file is analogous to the syntax of the `op0`-file except that it has only one column:

`# 1 X 7`	
K_1'	$[\beta_{\rm grid}]$
K_2'	$[\beta_{\rm grid}]$
μ_0'	[rad]
e'	
ω_0'	[rad]
ω_1'	$[{\rm rad}/P_{\rm ano}]$
q'	[1]

(`*.op1`)

The primes indicate that these are, in general, the optimized parameters. However, if only separation was run, or if a parameter was was given a zero Δ-value in the `op0`-file, its 'primed' value equals the one in the `op0`-file.

The optimized parameters of orbit deserve special discussion. Due to the un-constrained nature of the optimization technique one and the same orbital solution may be returned in various forms. For example μ_0 and/or ω_0 may be returned with values out of the expected range and one is allowed to add $\pm 2\pi$ as many times as necessary to each to bring them back. This transformation can be written as:

$$\begin{pmatrix} \mu_0' \\ \omega_0' \end{pmatrix} \longleftrightarrow \begin{pmatrix} \mu_0' + 2\,m\,\pi \\ \omega_0' + 2\,n\,\pi \end{pmatrix} \tag{4.2}$$

where m and n are integers. Less evidently, if FDBINARY returns the negative eccentricity the following transformation of the parameters of orbit can be applied:

$$\begin{pmatrix} e' \\ \mu_0' \\ \omega_0' \end{pmatrix} \longleftrightarrow \begin{pmatrix} -e' \\ \mu_0' \pm \pi \\ \omega_0' \pm \pi \end{pmatrix} \tag{4.3}$$

If both radial-velocity semi-amplitudes are returned negative:

$$\begin{pmatrix} K_1' \\ K_2' \\ \omega_0' \end{pmatrix} \longleftrightarrow \begin{pmatrix} -K_1' \\ -K_2' \\ \omega_0' \pm \pi \end{pmatrix} \tag{4.4}$$

Finally, in the no-light-variability case, the inspection of the parameters of orbit may show that FDBINARY swapped the components with respect to what one expects to get. In such case the model spectra may be swapped

back provided that the parameters of orbit are transformed according to:

$$\begin{pmatrix} x_{1i} \\ \vdots \\ x_{1N} \end{pmatrix} \longleftrightarrow \begin{pmatrix} x_{2i} \\ \vdots \\ x_{2N} \end{pmatrix} \quad \text{and} \quad \begin{pmatrix} K_1' \\ K_2' \\ \omega_0' \end{pmatrix} \longleftrightarrow \begin{pmatrix} K_2' \\ K_1' \\ \omega_0' \pm \pi \end{pmatrix} \tag{4.5}$$

The above transformation rules were derived by requiring the invariance of the radial velocities (A.11).

Only for convenience FDBINARY writes two additional files that do not contain any information independent of what was already output. The syntax of the `op2`-file is:

`# 5 X` M				
E_1'	μ_1'	Ω_1'	β_{11}'	β_{21}'
E_2'	μ_2'	Ω_2'	β_{12}'	β_{22}'
$\vdots$	$\vdots$	$\vdots$	$\vdots$	$\vdots$
E_M'	μ_M'	Ω_M'	β_{1M}'	β_{2M}'
$[P_{\rm sid}]$	[rad]	[rad]	$[\beta_{\rm grid}]$	$[\beta_{\rm grid}]$

(`*.op2`)

The optimized epochs, E_j' differ from the input epochs only if the correction to the sidereal period was optimized. $\Omega_j' = \omega_0' + \omega_1' E_j'$ is the longitude of periastron at epoch E_j'. The radial velocities β_{kj}' are pure Keplerian radial-velocities, i.e. they do not include the radial-velocity of the center-of-mass correction γ_j specified in the `des`-file. The 'complete' radial-velocities are written into the `op3`-file:

`# 5 X` M	
$\gamma_1 + \beta_{11}'$	$\gamma_1 + \beta_{21}'$
$\gamma_2 + \beta_{12}'$	$\gamma_2 + \beta_{22}'$
$\vdots$	$\vdots$
$\gamma_M + \beta_{1M}'$	$\gamma_M + \beta_{2M}'$
$[\beta_{\rm grid}]$	$[\beta_{\rm grid}]$

(`*.op3`)

Once again note that the `op2` and `op3`-files are redundant to `des` and `op1`-files (they do not contain new information).

4.4 The V453 Cyg example

In the Chapter 3 I have shown the results of disentangling of the observed spectra of the massive binary system V453 Cyg. All calculations were carried

out with FDBINARY. In this section I use the FDBINARY input and output matrixfiles of that work as examples.

The eight observed spectra are listed in the Table 3.1. The body of the `ecc.des` used with these spectra was:

```
# 5 X 8
# descriptors to spectra of V453 Cyg (H gamma) A&A 281 286
# phase     rv0     lf1        lf2        wght  label
# [1]       [pix]
  0.17663   0       0.727273   0.272727   1     #  b
  0.21827   0       0.727273   0.272727   1     #  e
  0.41941   0       0.727273   0.272727   1     #  c
  0.50625   0       1.000000   0.000000   1     #  f ECL!
  0.68875   0       0.727273   0.272727   1     #  d
  0.71775   0       0.727273   0.272727   1     #  g
  0.75397   0       0.727273   0.272727   1     #  h
  0.92208   0       0.727273   0.272727   1     #  a
# end of file (ecc.des)
```

The epochs (first column) are calculated according to (3.1). There was no need to use γ_j corrections (second column) because the observed spectra were corrected for the barycentric velocity (motion of Earth around the center of mass of the Solar system). The light-factors are assigned to the observed spectra according to (3.2), see also discussion to (3.3). All spectra were weighted equally (fifth column)

The body of the `ecc.obs` is too large to be included here. Its first line indicates the size of the data set, while the next lines contain a comment regarding the origin and wavelength range of the spectra:

```
#  8  X  1344
#  Observed spectra of V453 Cyg (H gamma) A&A 281 286
#  Sampled logarithmically in wavelength 4297.00 A to 4493.86 A
```

Since wavelengths are not part of the body of the matrixfile it is wise to note the wavelengths of the first and of the last data bin in the grid, as in the example above. The radial velocity resolution of the grid can easily be reconstructed as follows:

$$\beta_{\rm grid} = \frac{c\,\ln(\lambda_N/\lambda_1)}{N-1} = \frac{c\,\ln(4493.86/4297.00)}{1344-1} = 10\ {\rm km\,s^{-1}}\ . \qquad (4.6)$$

The parameters of orbit were initialized only very roughly in accord with the expected values. The five parameters that were optimized were assigned large range halfwidths. The file `ecc.op0` is:

```
# 2  X  7
# initial orbital parameters and ranges for V453 Cyg
# assumed radial velocity resolution 10 km/s
# value     range hw              interpretation
   20.0       4.0            #   160 km/s  <  K1  <  240 km/s
   20.0       4.0            #   160 km/s  <  K2  <  240 km/s
  1.5708     3.1416          #   90 deg +/- 180 deg (full cycle)
   0.05       0.05           #   0  <  eccentricity  <  0.1
   0.00      3.1416          #   0 deg +/- 180 deg (full cycle)
    0          0             #   apsidal motion not considered
    0          0             #   sidereal period not optimized
# end of file (ecc.op0)
```

FDBINARY was run with the following command line:

```
$ fdbinary mode=op runid=ecc nruns=36
```

The file `obs.op1` contains the optimized parameters of orbit:

```
#  1  X  7
 1.744781E+01
 2.162759E+01
 4.179180E+00
-2.253196E-02
-2.641274E+00
 0.000000E+00
 0.000000E+00
```

This orbital solution is shown in the Table 3.2 with the label 'use all' (because all eight observed spectra were used). Note that in this example the eccentricity (fourth data line) was returned negative so that, according to (4.3), μ_0 and ω_0 had to be shifted by $\pm\pi$. The spectra resulting from this run are shown in Figure 3.2, upper panel, and in Figures 3.4 and 3.5.

For the no-light-variability run the `des`-file was changed to:

```
# 5 X 8
# descriptors to spectra of V453 Cyg (H gamma) A&A 281 286
# N O   L I G H T   V A R I A B I L I T Y   R U N
# in-eclipse spectrum weighted out, generic light factors
# phase     rv0     lf1   lf2     wght  label
# [1]       [pix]
  0.17663   0       0.5   0.5      1    #  b
  0.21827   0       0.5   0.5      1    #  e
```

```
  0.41941   0       0.5   0.5      1    #  c
  0.50625   0       0.5   0.5      0    #  f ECL!
  0.68875   0       0.5   0.5      1    #  d
  0.71775   0       0.5   0.5      1    #  g
  0.75397   0       0.5   0.5      1    #  h
  0.92208   0       0.5   0.5      1    #  a
# end of file (nolitevar.des)
```

Note that I did not have to remove the spectrum observed during the eclipse from the `obs`-file; it was sufficient to assign it zero weight in the `des`-file. The orbital solution obtained in this run is labeled 'skip f' in the Table 3.2. The quasi-spectra (the raw output `mod`-file, not yet renormalized) are shown in Figure 3.2, lower panel.

Chapter 5

Conclusion

The spectral separation and disentangling techniques (Bagnuolo & Gies 1991; Simon & Sturm 1994a; Hadrava 1995) have been successfully applied in the analyzes of dozens of close binary systems and are becoming more and more widely accepted (Hensberge et al. 2000; Fitzpatrick et al. 2002; Griffin 2002; Harries et al. 2002; Ribas et al. 2002; Fitzpatrick et al. 2003). Still, not all aspects of the methods are fully understood. The contribution of this work to the understanding and acceptance of the techniques can be summarized as follows:

- It is shown that the 'tomographic', 'wavelength-domain' and the 'Fourier-domain' separation techniques are in great part equivalent one to another. The differences among them are discussed and it is shown that the Fourier-domain approach is the simplest, but also the most limited.

- Disentangling of composite spectra is defined as an application of the spectral separation technique. It is made clear that any of the forementioned separation techniques can be used in a disentangling process.

- The singularity in the separation problem is shown to be a consequence of the no-light-variability assumption. The mathematically correct treatment of the component spectra obtained in this case is presented in the form of a 'renormalization procedure'.

- The application of the disentangling method on the spectra of V453 Cyg is shown in more detail than any other application of the method in the published literature. The 'renormalization procedure' is applied and it is shown to lead to correctly normalized spectra in the no-light-variability case.

- The code FDBinary written by the author is documented and can be used in further research.

I believe that this work will help to understand and further develop these promising techniques.

Appendix A

The equations of orbital motion

This appendix reviews the equations related to the motion of stars in a binary system. Only the quantities of interest in the context of separation of composite spectra are considered. In particular this is the time dependence of the radial velocities of the components of a binary system in eccentric orbits with and without the apsidal motion. Another important relation is that of the times of the eclipses to the position of the stars in the orbit. For the full treatment of the Kepler problem see Goldstein (1980), and for the physical interpretation of the apsidal motion see Claret & Gimenez (2001) or Hilditch (2001).

A.1 Keplerian orbit

As long as the component stars are understood as point masses the orbital motion is given by the solution to the Kepler problem. For simplicity I will be considering the trajectory of only one of the component stars which I call the 'primary'. The trajectory in the orbital plane with respect to the center of mass of the binary system written using polar coordinates r and ϑ is an ellipse:

$$r(\vartheta) = \frac{a(1-e^2)}{1+e\cos\vartheta}\,, \tag{A.1}$$

where a is the major semi-axis, and e is the eccentricity of the orbit. In the astronomical tradition the angle ϑ is known as the *true anomaly.* The star is closest to the center of mass when $\vartheta = 0$, this particular point in the orbit is known as the *periastron.*

To obtain the position in the orbit as the function of time the true

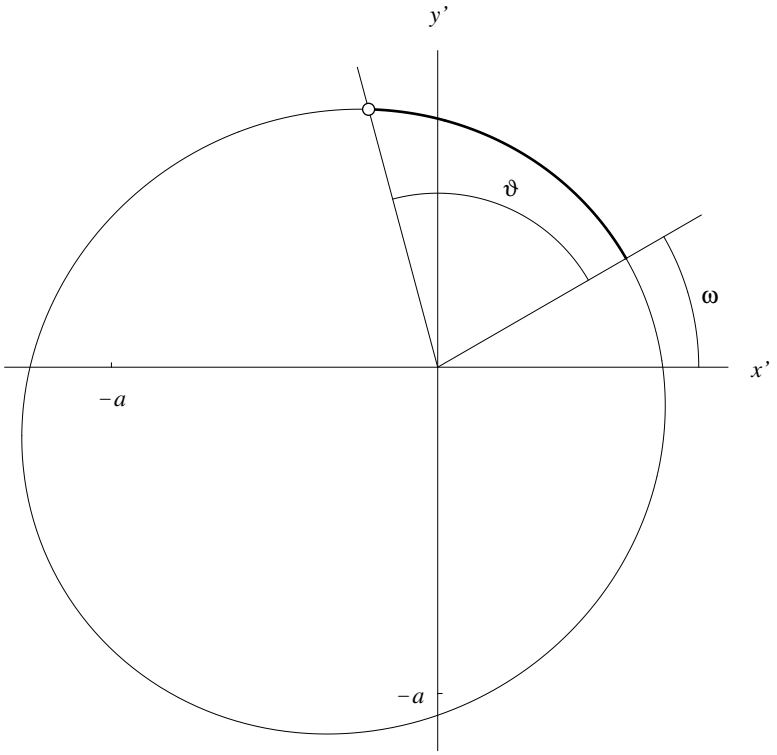

Figure A.1: The purely Keplerian orbit of a component in a binary system. The $x'y'$ plane is the plane of orbit with the angular momentum vector pointing upward. The center of mass (the focus of the ellipse) is at the origin of the coordinate system. The x' axis is the intersection of the plane of orbit and the plane of the Sky and the y' axis is the projection of the line of sight onto the plane of orbit with the observer at the negative end. On this drawing the eccentricity $e = 1/3$, longitude of periastron $\omega = \pi/6$, and the star is shown at the true anomaly $\vartheta = 5\pi/12$.

anomaly ϑ is firstly related to an auxiliary angle ψ, also known as the *eccentric anomaly.* The relation is:

$$\tan\frac{\psi}{2} = \sqrt{\frac{1-e}{1+e}}\tan\frac{\vartheta}{2}\ . \tag{A.2}$$

The eccentric anomaly is finally related to the *mean anomaly*, μ, an angle proportional to time:

$$\mu = \psi - e\sin\psi\ . \tag{A.3}$$

The epoch, E, is a dimensionless quantity proportional to time. It is defined to advance by unity over one orbital cycle of the binary system. Its integral part is the 'full cycle count', and the fractional part is the orbital phase. I may write:

$$\mu - \mu_0 = 2\pi(t-t_0)/P = 2\pi E \tag{A.4}$$

where μ_0 is the mean anomaly at epoch zero, i.e. at $t = t_0$. As (A.3), known as the *Kepler equation,* cannot be solved analytically for the eccentric anomaly ψ there is no analytical expression for $\vartheta(t)$.

The plane of orbit can have any orientation with respect to the line of sight. To specify this orientation only to the extent needed to explain the observed values I introduce the 'primed' coordinate system $x'y'z'$ as follows:

- the origin of the system is at the center of mass of the binary,
- the angular momentum vector points along the z' axis (it follows that $x'y'$ is the orbital plane),
- x' axis is (parallel to) the intersection of the plane of the Sky and the orbital plane and is oriented such that the star is receding from the observer when crossing its positive side (it follows that the y' axis is the projection of the line of sight onto the orbital plane, with the observer on the negative side.)

The trajectory is now:

$$\begin{pmatrix} x' \\ y' \\ z' \end{pmatrix} = r(\vartheta)\begin{pmatrix} \cos(\omega+\vartheta) \\ \sin(\omega+\vartheta) \\ 0 \end{pmatrix} \tag{A.5}$$

where $r(\vartheta)$ is given by (A.1) and the angle ω is the is known as the *longitude of periastron.* Note that the longitude of periastron of the secondary component is $\omega \pm \pi$. I can now write the orbit in a new (unprimed) coordinate system

xyz that is rotated with respect to $x'y'z'$ about the $x = x'$ axis by an angle i such that the z axis now points toward the observer. For the orbit I have:

$$\begin{pmatrix} x \\ y \\ z \end{pmatrix} = r(\vartheta) \begin{pmatrix} \cos(\omega + \vartheta) \\ \cos i \sin(\omega + \vartheta) \\ -\sin i \sin(\omega + \vartheta) \end{pmatrix} . \tag{A.6}$$

The angle i is known as the *inclination* of the orbit and is defined in this context as $0 \leq i \leq \pi$.

The real separation of the two stars $r(\vartheta)$ is given by (A.1). For $e > 0$ this function has one minimum at the periastron. The apparent separation is the projection of the real separation onto the plane of the Sky:

$$\rho^2(\vartheta) = x^2 + y^2 = r^2(\vartheta) \left(1 - \sin^2(\omega + \vartheta) \sin^2 i\right) \tag{A.7}$$

The apparent separation may have, depending on e, ω and i, one or two minima. Assuming the stars are spherical these minima may correspond to times of eclipses.[1] Substituting $\varphi = \vartheta + \omega$ into (A.7), differentiating with respect to φ, and equating to zero, one is looking for a solution to:

$$0 = e \cos^2 i \cos\omega \sin\varphi - \cos\varphi \left(\sin^2 i \sin\varphi + e \sin\omega\right) . \tag{A.8}$$

If expressed in terms of one trigonometric function of φ this turns out to be a fourth degree equation. Its roots can nonetheless be obtained analytically, but as the expressions are fairly complicated they are not useful in practice. For a low eccentricity orbit seen at high inclination all four roots of (A.8) are real. The two that are approximately at $\varphi_{1,2} = \omega + \vartheta_{1,2} \simeq \pm\pi/2$ correspond minima of ρ, and therefore to eclipses. At $\varphi \simeq \pi/2$ the primary star is eclipsed by the secondary, while at $\varphi \simeq -\pi/2$ it is the other way round.

The radial velocity (RV) of a star is the projection of the velocity of the star onto the line of sight. Positive RV is assigned to a receding star. Since z is the line of sight I have:

$$v_{\mathrm{rad}} = -\frac{\mathrm{d}z}{\mathrm{d}t} = -\frac{\partial z}{\partial \vartheta}\frac{\mathrm{d}\vartheta}{\mathrm{d}t} \tag{A.9}$$

Using (A.1) I obtain

$$v_{\mathrm{rad}} = r^2\dot{\vartheta}\frac{\sin i}{a(1-e^2)}(\cos(\omega + \vartheta) + e\cos\omega) \tag{A.10}$$

[1] For given e, ω and i the system may or may not exhibit eclipses. Assuming spherical stars, the condition for existence of an eclipse is that the projected separation of the stars at its minimum is smaller than the sum of the stellar radii.

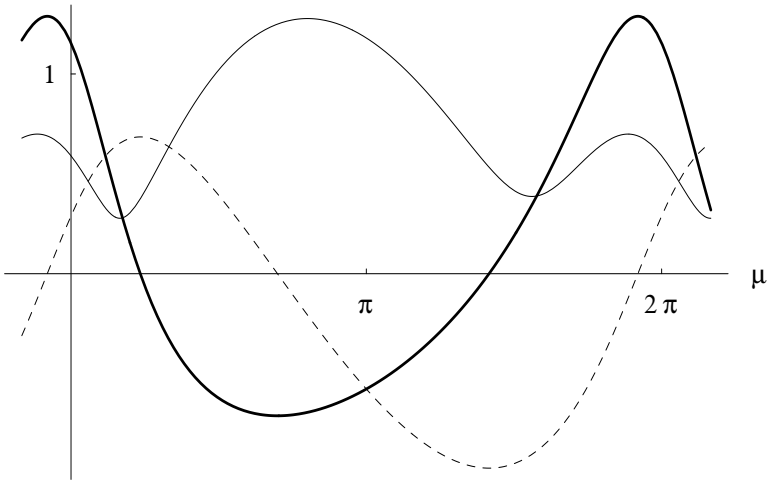

Figure A.2: Radial velocity (A.11; $K = 1$) (*thick line*), radial distance (A.6, $-z$; $a = 1$) (*dashed*) and the separation projected onto the plane of Sky (A.7; $a = 1$) (*thin*) as functions of the mean anomaly μ (phase since periastron passage) for the orbit of Fig. A.1 at the inclination of $i = \pi/3$.

The quantity $r^2\dot{\vartheta}$ is recognized as the angular momentum per unit mass and can be written as $2A/P$ where A is the area of the orbit and P the orbital period.[2] Finally:

$$v_{\rm rad} = K\,(\cos(\omega + \vartheta) + e\cos\omega) \tag{A.11}$$

where K is known as the *radial velocity semi-amplitude:*

$$K = \frac{2\pi a \sin i}{P\sqrt{1-e^2}}\,. \tag{A.12}$$

The radial velocity (A.11) has a maximum at $\omega + \vartheta = 0$ and a minimum at $\omega + \vartheta = \pi$. These points correspond to intersections of the trajectory and the x axis, and are known as ascending and descending node.

A.2 Circular approximation

In addition to the orbital period of the binary system, five parameters are required to specify the radial velocities and the times of the minima of the stars in an eccentric orbit ($K_{1,2}$, μ_0, e and ω), while only three are necessary in a circular orbit ($K_{1,2}$ and μ_0). At low orbital eccentricity the longitude

[2]Proof: $r^2\dot{\vartheta} = \frac{1}{P}\int_0^P r^2\dot{\vartheta}\mathrm{d}t = \frac{1}{P}\int_0^{2\pi} r^2\mathrm{d}\vartheta = \frac{2A}{P}$

of periastron ω becomes correlated with the overall phase shift μ_0 and only the sum of the two can be well determined. Therefore, one is tempted to use circular orbit as an approximation in order to diminish the number of free parameters. However, it is important to be able to estimate the level at which the radial velocities are affected by the 'circular approximation'. I therefore compare the radial velocities in a low eccentricity orbit to those in a closest circular orbit.

To make the treatment simpler I first introduce the 'low eccentricity approximation'. If $e \ll 1$ I expect $\vartheta \simeq \psi \simeq \mu$. Within this approximation the Kepler equation (A.3) can be inverted:

$$\psi \simeq \mu + e \sin \mu \ . \tag{A.13}$$

Similarly (A.2) can be approximated by:

$$\vartheta \simeq \psi + e \sin \psi \qquad \text{or} \qquad \psi \simeq \vartheta - e \sin \vartheta \ . \tag{A.14}$$

Using (A.3), (A.13) and (A.14), and keeping only the terms linear in e, I get:

$$\vartheta \simeq \mu + 2e \sin \mu \qquad \text{or} \qquad \mu \simeq \vartheta - 2e \sin \vartheta \tag{A.15}$$

Thus the low eccentricity approximation ($\vartheta \simeq \psi \simeq \mu$) allowed me to write the approximate analytical expression for the dependence of ϑ on μ.

Within the low eccentricity approximation the radial velocity of a star $v_{\rm rad.}$ can be written as a function of μ. Using (A.11) and (A.15):

$$v_{\rm rad.}^{(e \ll)} = K \left(\cos(\omega + \mu) - 2e \sin \mu \sin(\omega + \mu) + e \cos \omega \right) \ . \tag{A.16}$$

The general form of the radial velocity of a star in a circular orbit with the same period can be written as:

$$v_{\rm rad.}^{(e=0)} = K' \cos(\mu + \mu_0) \ . \tag{A.17}$$

where μ_0 plays the role of a phase shift. I now compute the least squares fit of $v_{\rm rad.}^{(e \ll)}$ to $v_{\rm rad.}^{(e=0)}$ by minimizing the quantity:

$$\begin{aligned} r^2 &= \int_0^{2\pi} \left(v_{\rm rad.}^{(e=0)}(\mu) - v_{\rm rad.}^{(e \ll)}(\mu) \right)^2 {\rm d}\mu \\ &= \pi \left(K'^2 + (1+e^2)K^2 - 2KK' \cos(\mu_0 - \omega) \right) \ . \end{aligned} \tag{A.18}$$

The minimum of r^2 is at $\mu_0 = \omega$ and $K' = K$, which means that, assuming uniform phase coverage, the circular approximation (A.17) introduces no bias into the radial velocity semi-amplitude K. The difference

$$v_{\rm rad.}^{(e=0)}(\mu) - v_{\rm rad.}^{(e \ll)}(\mu) = Ke \cos(2\mu + \omega) \ . \tag{A.19}$$

gives a constraint for the applicability of the circular approximation. If the individual radial velocities can be measured at precision comparable to this difference, which is of the order of Ke, the use of the circular approximation is no longer justified.

The eccentricity is most easily detected in binary systems exhibiting two eclipses. In a circular orbit the times of the two minima are half of the orbital period apart. If $e > 0$ and $\omega \neq \pm\pi/2$ this is no longer true. As noted in the discussion of the equation (A.8) the general solution to problem of the times of minima is straightforward but complicated. The situation is, however, much simpler within the low eccentricity approximation. Assuming that the minima occur at $\varphi_{1,2} \simeq \pm\pi/2$ the equation (A.8) can be expanded using $\varphi_{1,2} = \pm\pi/2 + \delta_{1,2}$. Keeping only the first two terms one obtains:

$$\delta_{1,2} = \mp e \, \cos\omega \, \cot^2 i \, \left(1 \mp e \, \sin\omega \csc^2 i\right) + O^3(e) \tag{A.20}$$

The true anomalies corresponding to the eclipses are $\vartheta_{1,2} = -\omega \pm \frac{\pi}{2} + \delta_{1,2}$. Corresponding mean anomalies can be obtained using (A.15). The quantity

$$\Delta\mu = \mu(\vartheta_2) - \mu(\vartheta_1) - \pi = 2e \, \cos\omega \, (1 + \csc^2 i) + O^2(e) \tag{A.21}$$

can be interpreted as the 'phase shift' of the secondary eclipse from its phase in a circular orbit, relative to the phase of the primary eclipse. This phase shift can be measured in the light curve and thus it provides a constraint on the eccentricity.

A.3 Apsidal motion

In presence of apsidal motion distinction is made between three different periods, although any two of them are sufficient to specify the rate of change of the longitude of periastron in time. The *apsidal period*, $P_{\rm aps}$, is the time it takes for the periastron to complete one revolution around the center of mass. The *anomalistic period*, $P_{\rm ano}$, is the time that elapses between two successive periastron passages. In binary stellar systems $P_{\rm aps} \gg P_{\rm ano}$. Denoting the number of periastron passages (anomalistic cycles) during one apsidal cycle with N (not necessarily an integer) I have $P_{\rm aps} = NP_{\rm ano}$. The *sidereal period*, $P_{\rm sid}$, is usually defined as the average time between eclipses of the same component, or the average time of one revolution (ignoring the periastron advance) in case of a non-eclipsing system. Assuming the line of apsides rotates in the sense of orbital motion I have:

$$P_{\rm aps} = NP_{\rm ano} = (N+1)P_{\rm sid} \tag{A.22}$$

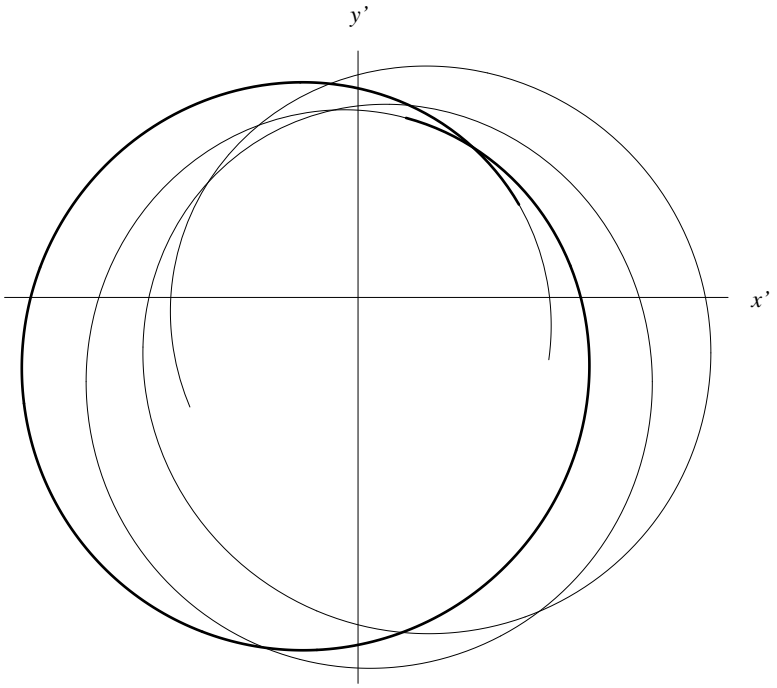

Figure A.3: A portion of the trajectory of a star in an eccentric orbit with apsidal motion. One complete anomalistic (periastron to periastron) cycle is indicated by the bold line. At the beginning of the bolded cycle the parameters of orbit coincide with the ones used in Fig. A.1. The longitude of periastron advance per sidereal cycle is in this figure $\omega_1 = 1/8$ (exaggerated by several orders of magnitude).

since there must be one more sidereal than anomalistic cycle during one apsidal cycle (note that the final result (A.25) will be valid for both senses of rotation of the line of apsides). The definition of the epoch (A.4) is modified so that the epoch advances by unity over one sidereal cycle. Accordingly, the periastron advance, ω_1, is usually expressed in the unit of one sidereal cycle:

$$\omega = \omega_0 + \omega_1 E \ , \tag{A.23}$$

where ω_0 is the longitude of periastron at $E = 0$. As there are $N+1$ sidereal cycles in one apsidal cycle I have:

$$(N+1)\omega_1 = 2\pi \ . \tag{A.24}$$

Combining the above relations the mean anomaly μ can be expressed in terms of the mean anomaly at $E = 0$ (or $t = t_0$), μ_0, and the periastron advance ω_1:

$$\mu - \mu_0 = 2\pi \frac{t - t_0}{P_{\rm ano}} = (2\pi - \omega_1) \frac{t - t_0}{P_{\rm sid}} = (2\pi - \omega_1) E \tag{A.25}$$

In presence of apsidal motion (A.4) is replaced by (A.25) which is valid for $\omega_1 > 0$ as for $\omega_1 < 0$. The Equations (A.7) and (A.11) can be used unmodified provided that the longitude of periastron ω is being continuously updated according to (A.23). Compared to an eccentric orbit without apsidal motion, the orbit with apsidal motion requires the same number of initial conditions, and only one additional parameter (common choice is ω_1).

Appendix B

The renormalization procedure

Component spectra reconstructed by spectral separation techniques are *not unique* if equal light contributions of the component stars to all composite spectra are assumed. Section 2.5 discusses the mathematical background, while this appendix proposes a procedure for treatment of component spectra to facilitate correct physical interpretation. The procedure is limited to the spectra of a binary system reconstructed through the system of equations of Section 2.4 and it treats only the 'additive constant' degree of freedom. The procedure allows bringing the component spectra into consistency with the trial light ratio without having to re-run the separation procedure.

If the separation is carried out using the so called 'generic light factors', $\ell_1 = \ell_2 = \ell_{\text{gen.}} = 1/2$ I obtain two quasi-spectra that I label z_{1i} and z_{2i}, $i = 1, \ldots, N$. Note that using the generic light-factors does not mean that I assumed equal light contribution of the component stars, the choice is only for later convenience. The quasi-spectra fit the data under generic light factors, but I can transform them into spectra that would fit the data under any other set of light factors. Assuming the light ratio L I have $\ell_1 = L/(L+1)$ and $\ell_2 = 1/(L+1)$. The spectra that would fit the data under these light-factors are:

$$x_{1i} = \frac{L+1}{2L}(z_{1i} + c) \qquad \text{and} \qquad x_{2i} = \frac{L+1}{2}(z_{2i} - c)\ , \tag{B.1}$$

where c is a free parameter. Any value of c results in the same fit to the data, but not necessarily with the physically meaningful spectra. The requirements that might help constrain the allowed range of values of c could be:

- x_{1i} and x_{2i} should be positive at all wavelengths (except in extreme cases when the faint component becomes so affected by random noise that I must allow protruding into negative amplitudes) and
- in the continuum regions the amplitudes should not systematically ex-

ceed unity (random noise and emission regions are however allowed to exceed unity).

The first requirement is more useful with components with numerous and deep absorption lines (late spectral types), while the second one is more useful with stars with few broad absorption lines and wide continuum regions (early spectral types). It turns out that, other than these two requirements that only impose absolute limits on the physically acceptable value of c, there is no objective way of obtaining its value. It must be obtained by trial and error until *both* spectra look acceptable.

The free parameter c in (B.1) can be related to a physical quantity in order to make adjusting easier. The average of the amplitudes, i.e. the zero-frequency components of the DFTs, of the amplitudes in the quasi-spectra are according to (2.19):

$$\tilde{z}_{10} = \tilde{z}_{20} = \frac{\sum_j \sigma_j^{-2} \tilde{y}_{j0}}{\sum_j \sigma_j^{-2}} = 1 - b \; . \tag{B.2}$$

This means that that they are equal to the weighted average of the amplitudes in the composite spectra. The quantity b is defined as the weighted *line-blocking* in the composite spectra or in the quasi-spectra. In addition I define the *line blocking ratio*, B, as the ratio of the average line-blockings in the two component spectra:

$$B = \frac{1 - \tilde{x}_{10}}{1 - \tilde{x}_{20}} \; . \tag{B.3}$$

With a little algebra the free parameter c can be expressed in terms of L, b and B:

$$c = \frac{L - 1}{L + 1} - \frac{BL - 1}{BL + 1} b \tag{B.4}$$

The renormalization procedure can now be organized as follows:

1. Calculate the quasi-spectra z_{1i} and z_{2i} using the generic light-factors $\ell_1 = \ell_2 = \ell_{\text{gen.}} = 1/2$.

2. Calculate the weighted line blocking in the composite spectra b (easiest by calculating the line-blocking in any of the quasi-spectra).

3. Decide on trial values of the light ratio L and the line blocking ratio B and compute the value of the free parameter c using eq. (B.4). The light ratio L is hopefully constrained by the photometry, while for not too different spectral types of component stars a reasonable first guess for the line-blocking ratio is $B = 1$,

4. Use (B.1) to calculate the component spectra z_{1i} and z_{2i} in accord with B and L used in step 3. Examine *both* component spectra and if necessary return to step 3 and use adjusted values of B and L. Taking a higher (lower) B pushes x_1 down (up)and x_2 up (down).

It could be argued that introducing line-blockings is an unnecessary complication beyond (B.1). The reason for introducing b and B is that it is much safer to be adjusting a quantity with a clear physical interpretation then a mere mathematical construct.

Abstract

Disentangling of composite spectra is a data analysis technique that can be applied to a time-series of observed spectra of a double lined spectroscopic binary star to simultaneously optimize the parameters of the orbit and reconstruct the spectra of its component stars. The key feature of this technique when compared to the predcessors (eg. cross-correlation or spectral subtraction) is that it does not rely on the template spectra. Rather, the amplitudes of the spectra of component stars are modeled through a large scale linear least squares fit to the observed spectra. The underlying spectral separation algorithm reconstructs the best-fit component spectra consistent with the supplied orbital radial velocities and the light-ratio. The disentangling technique goes one step further by including the parameters of orbit into the parameters of the fit, thus obtaining the self-consistent solution. The radial velocity semiamplitudes obtained through disentangling are more accurate than those obtained with the traditional techniques and lead to more accurate determinations of the masses of the component stars. The reconstructed spectra of component stars can be analyzed with the methods developed for the spectra of single stars. In this work I discuss the mathematical background of the separation and disentangling techniques. I elaborate in detail the formulations of the separation problem in the wavelength domain and in the Fourier domain, paying attention particularly to the physically correct normalization of the component spectra that are obtained. As an example I have applied the disentangling technique to the time series consisting of eight optical spectra of the hot massive binary V453 Cyg. I have also documented the computer code for disentangling and separation of the composite spectra that I developed and used.

Acknowledgements

I am deeply indebted to my supervisor, Prof. Krešimir Pavlovski (University of Zagreb), who invited me to join his research group in 1999 and provided his support and guidance while I worked on my thesis. Dr. Herman Hensberge (Koninklijke Sterrenwacht van België) made my three research visits to KSB possible, and has greatly contributed to my understanding of stellar spectroscopy. Lars Michael Freyhammer (Vrije Universiteit Brussel and KSB) was the first astronomer who run my disentangling codes and his comments and suggestions were very helpful to me. I would like to thank the architects of the disentangling method, Dr. Petr Hadrava (Ondřejov Observatory) and Dr. Klaus Simon (Universitäts-Sternwarte, München), who were kind enough to find time and discuss matters with me. I am especially grateful to Dr. Klaus Simon for allowing me to use the spectra of V453 Cyg that are historically related to the introduction of the method, and provide the basis for Chapter 3 of this thesis.

Although they are not directly involved with the disentangling and separation techniques, I would like to thank Branimir Dolički whose books were on my desk most of the time, my colleague Ettore Tamajo for his humor and support, Prof. Ulisse Munari (Osservatorio Astrofisico, Asiago) who introduced me to the 182 cm telescope *Copernico* on Cima Ekar, Asiago, and Dr. Slobodan Danko Bosanac (Institute Ruđer Bošković, Zagreb) who enabled me to attend the *2002 Brijuni Conference, Space, Time and Life*. Most of the technical work I did during the quiet mornings in the room 78 of the Faculty of Geodesy in down-town Zagreb.

My family has been with me all the time.

Saša Ilijić,
`silijic@phy.hr`
Zagreb, Feb. 2003.

Bibliography

Bagnuolo W. G., Gies D. R., 1991, ApJ, 376, 266

Bagnuolo W. G., Gies D. R., Wiggs M. S., 1992, ApJ, 385, 708

Bíró I. B., 1998, IBVS 4555 (see errata to IBVS 4555 and 4633)

Burkholder V., Massey P., Morrell N., 1997, ApJ, 490, 382

Claret A., Gimenez A., 2001, in Lázaro F. C., Arévalo M. J., Binary Stars: Selected Topics on observations and Physical Processes, Lecture Notes in Physics 563, Springer, p. 1

Cohen H. L., 1971, PASP, 83, 677

Cohen H. L., 1974, A&AS, 15, 181

Efron B., 1982, The Jackknife, the Bootstrap and Other Resampling Plans, Society for Industrial and Applied Mathematics, Philadelphia

Fitzpatrick E. L., et al. 2002, ApJ, 564, 260

Fitzpatrick E. L., Ribas I., Guinan E. F., Maloney F. P., Claret A, 2003, `arXiv:astro-ph/0301296`

Gies D. R., Penny L. R., Mayer P., Drechsel H., Lorenz R., 2002, ApJ, 574, 957

Goldstein H., 1980, Classical Mechanics, 2nd ed., Addison-Wesley Publishing Company, Reading MA, etc.

Griffin R. E. M., 2002, AJ, 123, 988

Hadrava P., 1995, A&AS, 114, 393

Hadrava P., 1997, A&AS, 122, 581

Harries T. J., Hilditch R. W., Howarth I. D., 2002, arXiv:astro-ph/0210295

Hensberge H., Pavlovski K., Verschueren W., 2000, A&A, 358, 553

Hilditch R. W., 2001, An Introduction to Close Binary Stars, Cambridge University Press, Cambridge

Hynes R. I., 1996, Synthetic Spectra of OB-Type Binary Stars, A tool to Test the Disentangling Technique, MSc thesis, University of Sussex

Hynes R. I., Maxted P. F. L., 1998, A&A, 331, 167

Ilijić S., Hensberge H., Pavlovski K., 2001a, in Boffin H., Cuypers J., Steegs D., eds, Astrotomography: Indirect Imaging Methods in Observational Astronomy, Lecture Notes in Physics 573, Springer, p. 267.

Ilijić S., Hensberge H., Pavlovski K., 2001b, Fizika B, 10, 357

Johnson S., Frigo M., 1999, The FFTW Reference Manual (v.2.1.3), http://www.fftw.org

Popper D., Hill G., 1991, AJ, 101, 600

Press W. H., Teukolsky S. A., Vetterling W. T., Flannery B. P., 1992, Numerical Recipes in FORTRAN, 2nd ed., Cambridge University Press, Cambridge

Ribas I., et al. 2002, ApJ, 574, 771

Simon K. P., 2001, priv. comm.

Simon K. P., Sturm E., 1992, in Grosbøl, P. J., de Ruijsscher, R. C. E., eds, Proc. of the 4th ESO/ST-ECF Data Analysis Workshop, ESO, p. 91.

Simon K. P., Sturm E., 1994a, A&A, 281, 286

Simon K. P., Sturm E., 1994b, A&A, 282, 93

Simon K. P., Sturm E., Fiedler A., 1994, A&A, 292, 507

Thorstensen J., 2001, SkyCalc User's Manual (V5), Dartmouth College ftp://iraf.noao.edu/contrib/skycal.tar.Z

Sturm E., 1994, Spektralanalyse der Komponenten massereicher Doppelsterne, PhD thesis, Ludwig-Maximilians-Universität, München

Wachmann A. A., 1939, Astron. Nachr., 21, 136

Wachmann A. A., 1973, A&A, 25, 157

Wachmann A. A., 1974. A&A, 34, 317

Wolfram S., 1991, Mathematica: A System for Doing Mathematics by Computer, Addison Wesley Publishing Company